Rheology and Viscoelasticity of Proteins and Nucleic Acids Condensates

Davide Michieletto* and Mattia Marenda

Read Online

ACCESS | Metrics & More | Article Recommendations

ABSTRACT: Phase separation is as familiar as watching vinegar separating from oil in vinaigrette. The observation that phase separation of proteins and nucleic acids is widespread in living cells has opened an entire field of research into the biological significance and the biophysical mechanisms of phase separation and protein condensation in biology. Recent evidence indicates that certain proteins and nucleic acids condensates are not simple liquids and instead display both viscous and elastic behaviors, which in turn may have biological significance. The aim of this Perspective is to review the state-of-the-art of this quickly emerging field focusing on the material and rheological properties of protein condensates. Finally, we discuss the different techniques that can be employed to quantify the viscoelasticity of condensates and highlight potential future directions and opportunities for interdisciplinary cross-talk between chemists, physicists, and biologists.

KEYWORDS: *phase separation, condensates, viscoelasticity, complex fluids, rheology, nucleic acids, intrinsically disordered proteins, gels*
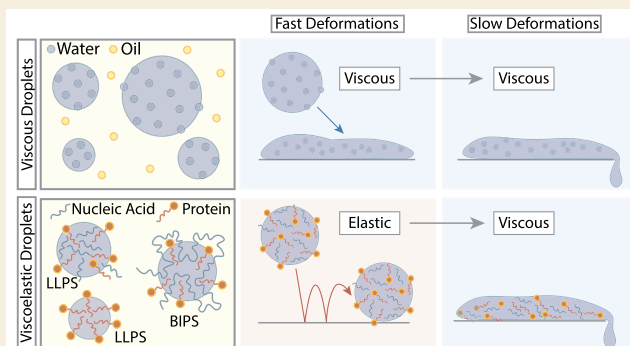
PHASE SEPARATION AND RHEOLOGY

In biology textbooks, organelles are defined as regions of space in the cell dedicated to specific operations such as the endoplastic reticulum, mitochondria, or the Golgi apparatus.[1] These physical compartments are characterized by a surrounding membrane that separates them from the rest of the cellular space. At the same time, there exist many examples of cellular compartments that are not surrounded by a membrane. The observation of membraneless compartments dates back to early 1900 with the sketches of Ramon y Cajal discovering the eponymous bodies[2,3] (Figure 1a). However, the realization of how widespread these membraneless compartments are arrived much more recently and encompasses a range of cell bodies, from the nucleolus[4] to germline granules[5] (see Figure 1b,c).

It is now broadly accepted that a wide range of proteins and nucleic acids (e.g., DNA and RNA) form membraneless compartments. Arguably, one of the most important and open questions in biology is to understand their biological significance and the biophysical mechanisms that drive their formation.[6−10] Although existing evidence suggests that liquid−liquid phase separation (LLPS)[11] (defined as a reversible thermodynamic process leading to the demixing of liquid fluids) is widespread and underlies the emergence of membraneless compartments, it has also been recently shown that some condensates exhibit puzzling and exotic flow behaviors and are far from being simple liquids.[12−15] As we

shall discuss in detail in this review, some proteins and nucleic acids condensates display so-called viscoelastic, i.e., both viscous and elastic, flow properties akin to those of gels, foams, or even rubbers.[16−19] These nontrivial behaviors may be due to (i) the so-called "ageing" of the fluid as consequence of LLPS-driven local increase in protein density,[13,20] (ii) the onset of percolating networks of associative "sticker-spacer" polymers,[14,15,21,22] or (iii) alternative demixing mechanisms, such as bridging-induced phase separation (BIPS)[23,24] (see Models of Phase Separation for a detailed discussion). In fact, while some protein condensates may display classic hallmarks of "liquid−liquid" phase separation such as fusion, they can either mature into solid-like structures or display subtler elastic behaviors at subsecond time scales once the high density phase is formed.[4,13,14,25] Thus, a condensate that originally formed by LLPS is not necessarily purely liquid at all times, and evidence of viscoelastic behaviors is increasingly more common. Importantly, the unexpected flow behaviors observed in certain condensates are thought to be biologically relevant and
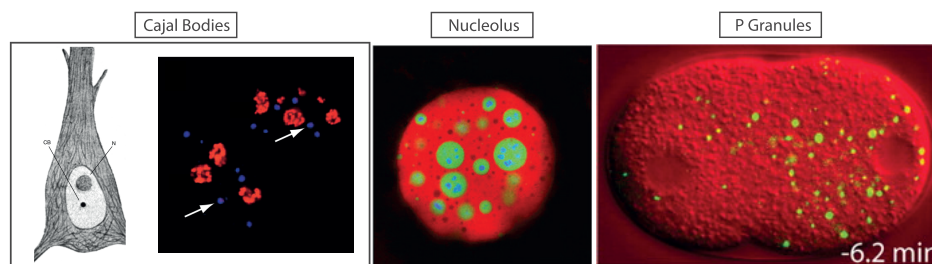
Figure 1. Examples of membraneless organelles. From left to right: Cajal Bodies as sketched by Ramon y Cajal (reproduced with permission from ref 30. 2003 Cell Press) and imaged in HeLa cells stained for coilin (blue) and fibrillarin (red) (reproduced with permission from ref 31. 2007 PLOS). The nucleolus of *X. laevis* stained for NPM1 (red), FIB1 (green), and POLR1E (blue) (reproduced with permission from ref 4. 2016 Cell Press). Germline P Granules expressing GFP::PGL-1 (green) on differential interference contrast (red) *C. elegans* (reproduced with permission from ref 5. 2009 AAAS).
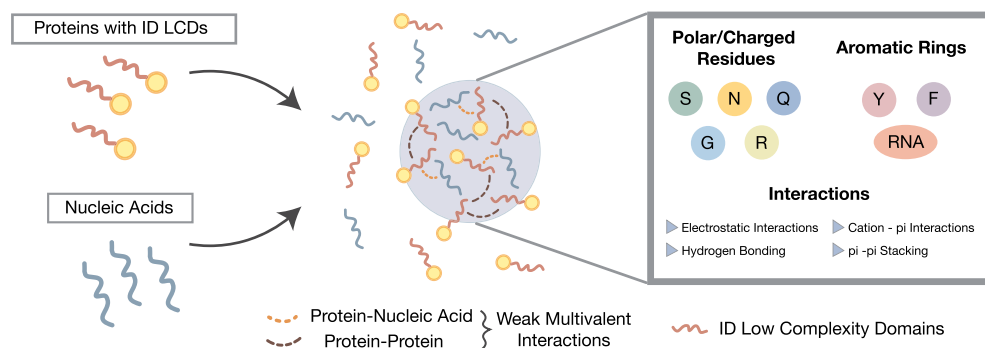

Figure 2. Biochemical interactions driving LLPS. Proteins containing Intrinsically Disordered Low Complexity Domains (ID LCDs) and nucleic acids are prone to phase separate into membraneless condensates. The drivers for such behavior are weak multivalent interactions, e.g., between proteins or proteins and nucleic acids, and involve polar/charged residues and aromatic rings in the protein residues and RNA. Protein−RNA interactions are typically electrostatic attractions and cation−π interactions. Protein residues typically interact through electrostatic interactions, hydrogen bonding, cation−π, and π−π stacking.

intimately related to certain diseases[26−28] or biological functions.[29]

To better understand the biological significance of phase separation *in vivo* it is therefore important to be able to quantitatively assess the material and flow properties of protein condensates. Rheology (from "panta rei" or "everything flows", a famous quotation of Heraclitus' philosophy) is a well-established research field with strong ties to polymer physics and soft matter but perhaps less broadly known by the biological and biochemical research communities. In this Perspective, we thus aim to provide a comprehensive yet synthetic overview of concepts and techniques that can be used to quantify the rheology and viscoelasticity of protein and nucleic acids condensates with the aim of assisting the design and interpretation of existing and future experiments in this field.

Biophysics and Biochemistry of Phase Separation

For liquids such as oil and water, demixing is driven to hydrophobic interactions: it is energetically favorable for water molecules to be surrounded by other water molecules as it creates the conditions for hydrogen bond formation, in turn reducing the internal energy of the system. These interactions overcome the entropy of mixing, which would tend to keep the oil and water molecules mixed throughout the solution. The thermodynamics of this process is described at the mean field level by Flory−Huggins (FH) theory,[16,32] even in the case where long polymers such as nucleic acids are involved in the process. In the simplified FH framework, the effective interaction strength is given by the so-called "Flory parameter" χ which captures how favorable polymer−polymer interactions are with respect to solvent−polymer ones. When χ is larger than a critical value χ_c, the system favors demixing. While the Flory parameter depends on the specific details of the system, its temperature, pH, etc. at mean field level χ_c only depends on the length of the polymers as it separates the regions where the enthalpic contributions win over the entropic ones.

This simple picture fails for protein condensates since the details of the protein sequence matter, and thus, refinement of the FH theory[33] or simulations with specific interactions[9] are necessary. The specific biochemical interactions and dependence on sequence composition that drive protein condensation, or in some cases co-condensation with nucleic acids, are not fully understood. Typically, protein condensation is driven by multivalent weak interactions between intrinsically disordered low-complexity domains (ID LCDs) of the protein, i.e., protein segments containing significant enrichment with specific amino acids types or sequence repeats,[34,35] and that do not adopt a unique folded conformation.[36,37] It is typically assumed that ID LCDs that have an enrichment in polar amino acids, such as serine, asparagine, glutamine, and glycine, have the potential to collapse and aggregate.[38−41] In particular, this seems to be more common if the strands of these polar amino acids are alternated by aromatic (tyrosine and phenylalanine) and charged (arginine) amino acids.[42] Both the patterning and the sequence position play a role in the phase separation, but few general principles have been uncovered (for a detailed review on molecular interactions and multicomponent

Table 1. Table of Viscosity η, Surface Tension γ, and Elasticity G'_p (Extracted from the Maximum Frequency That Could Be Measured in the Cited Work) for Different Natural and Synthetic Protein Condensates[a]

protein/body	η (Pa s)	γ (μN/m)	G'_p (Pa)	probes/method	refs
Human Nucleus	0.001−0.003			GFP FCS	70
Mouse Nucleus	25.1		0.48	MR, 200 nm nanorods	71
Mouse Nucleus	52		18	MR, 100 nm	72
Human Nucleus	1200		250	MR, 1 μm	73
Human Nucleus	3000			shape fluctuations	74
Human Nucleolus		1		shape fluctuation	74
X. laevis Nucleolus	12−32	0.4		coalescence	4
NPM1	0.74		no	MR, 50 nm	4
C. elegans P granules	1	1		coalescence	5
TDP-43	0.01−3.7			coalescence	75
LAF-1	8−34	100		coalescence/MR, 100 nm	39
LAF-1 RGG	1.62	159		micropipette aspiration	76
PGL-3 (75 mM KCl)	1	5	15	active MR, 1 μm	69
PGL-3 (180 mM KCl)	0.1	1	0.1	active MR, 1 μm	69
PGL-3 (early, 75 mM KCl)	4.4	4.5	56	active MR, 1 μm	13
PGL-3 (late, 75 mM KCl)	40	19.3	50	active MR, 1 μm	13
FUS (early)	4		0.4	active MR, 1 μm	13
FUS (late)	50		0.1	active MR, 1 μm	13
FUS	0.01−0.1			FRAP in vivo	77
FUS	1	100	no	sessile drop/MR, 100 nm	78
$[KGKGG]_5 - rU_{40}$	0.26		no	passive MR, 200 nm and 1 μm	14
$[RGPGG]_5 - rU_{40}$	0.1		no	passive MR, 200 nm and 1 μm	14
$[RGRGG]_5 - rU_{40}$	6		60	passive MR, 200 nm and 1 μm	14
water	0.001	72000	no		
honey	10	50000	10−100		

[a]Generic values for water and honey are given as reference. MR stands for microrheology. Unless specified, the probes for microrheology are spherical particles of given size. The G'_p table entry is marked as "no" if no elasticity was observed and otherwise "−" if not measured.

condensates, see ref 43). A specific subset of ID LCDs that has been extensively studied is the so-called RG/RGG protein domain.[44] This is a disordered RNA-binding domain present in several nuclear proteins, such as FUS protein, that shows repeats in arginine-glycine (RG) and arginine-glycine-glycine (RGG) sequences.[45] The typical interactions that have been suggested to occur in RGG phase separation include electrostatic interactions, cation−π, π−π, and hydrogen-bonding interactions[44] (see Figure 2). In these cases, glycine and diglycine residues have an exposed peptide bond in the backbone which promotes π−π interactions. The same amino acids may also form the π−π stacking with the arginine positively charged guanidino group as well as with aromatic side chains of tyrosine and phenylalanine.[33,46] Additionally, arginines are highly positively charged amino acids and can interact electrostatically with negatively charged or phosphorylated residues as well as with RNA molecules phosphate groups.[47−50] Interestingly, mutation of arginine to lysine on the RGG domain of Lsm4 protein has been shown to impair the ability of Lsm4 to form condensed P-Bodies.[51] The patterning of arginine is crucial, as both experiments and simulations suggest that the distribution of charges is a key factor that determines the dynamics of phase separation and the material properties of the condensates.[38,52,53] Arginine can also promote condensation mediated by cation−π interactions with aromatic residues, such as tyrosine and phenylalanine, and aromatic rings on RNA bases.[54,55] The removal of aromatic residues, and in particular of tyrosine, from an engineered FUS-like intrinsically disordered domain displays impaired phase separation.[42]

Besides the sequence composition of intrinsically disordered domains, condensate formation can be affected by environmental conditions such as temperature, ionic strength, pH, etc. as well as interactions between folded and disordered domains of the same protein.[56,57] A typical example is the RNA-binding protein hnRNPA1, where the presence of folded domains reverses the salt dependence of the driving force for phase separation.[58] Another intriguing case is that of hnRNPU, an abundant nuclear protein which does not display evidence of phase separation in spite of its RNA-binding domain being an RGG repeat similar to FUS and hnRNPA1.[59−61] Thus, current evidence suggests that protein condensation is not only due to the intrinsically disordered domains of proteins but also how they interact with the folded, structured domains.

VISCOELASTICITY OF CONDENSATES

As opposed to water—a so-called "Newtonian" fluid whose viscosity does not change as a function of the applied stress—many protein condensates (or proteins and nucleic acids co-condensates) are not simple liquids; rather, they are complex fluids with non-Newtonian behaviors.[13−15] Non-Newtonian fluids are characterized by the fact that their deformation rate is not trivially proportional to the amount of stress applied, or in other words, their viscosity depends on how much and how fast the sample is stressed.[62] For instance, shear-thinning fluids such as shampoos, creams, and ketchup display a lower viscosity when stressed and will thus flow more easily when spread over a surface. On the other end of the spectrum, shear thickening fluids such as oobleck (water and cornstarch) are more difficult to deform when quickly sheared. Other examples are yield stress materials, such as mayonnaise or shaving foam,

which require a threshold stress to be attained before they start to flow at all. In general, viscoelastic fluids display viscous and elastic responses that are nontrivial functions of the time scales (or frequencies) of the perturbations at which they are subjected to. For instance, an interesting class of viscoelastic fluids called Maxwell fluids display a single relaxation time scale τ_R. At deformation frequencies larger than τ_R^{-1} (fast deformations), the fluid behaves like an elastic solid, and at frequencies much smaller than τ_R^{-1} (slow deformations) it behave as a liquid.[13,14]

While LLPS is now widely argued to be involved in a range of fundamental biological processes such as gene expression,[63−66] the hypothesis that non-Newtonian properties of condensates may play a role in the cell biology has emerged only recently. For instance, a viscous liquid-like compartment could act as a protein reservoir or crucible to accelerate biochemical reactions.[64,67] On the contrary, elastic and gel-like RNA-protein condensates may offer local structural support to shape chromatin organization in the nucleus,[59,68] something that cannot be achieved by purely viscous condensates. At the same time, some material properties of protein condensates may have an impact on the cell health; for example, cytoplasmic appearance of stress granules formed by heterogeneous ribonucleoproteins such as hnRNPA1 and solid-like elastic fibrous structures are commonly observed in degenerative diseases such as amyotrophic lateral sclerosis, suggesting that the onset of solid-like properties of these condensates may be linked to the onset of the disease.[18,26]

Quantitative studies on the viscoelasticity of protein condensates has started only very recently.[13−15,69] To provide the reader with an overview of the typical values of viscous and elastic properties, we report a list of different proteins and nucleic acids condensates with their values of, where available, viscosity, surface tension, and elasticity (see Table 1). The table should also give the reader a sense of the heterogeneity in the values measured for similar condensates in the literature. As we shall explain in detail in the next section, these measurements are sensitive to the technique and probes employed. For instance, while small particles and GFP molecules are more suited to be embedded into cells and cell nuclei, they may be smaller than the pore or mesh size of their surrounding environment—around 10−100 nm for chromatin[70,79] compared with ≲10 nm of a GFP molecule, and therefore, may not fully capture the viscosity and elasticity of the bulk environment. A glaring example is the apparent viscosity of the nucleus found to be comparable to that of water by performing FCS on GFP molecules[70] and 3 million times larger using nuclear shape fluctuations.[74] In the next section, we will describe the different techniques that can be used to measure the viscoelastic behavior of protein and nucleic acids condensates.

Microrheology

Classical bulk rheology is typically performed on large samples by placing around 1 mL of sample in between plates that are made to rotate relative to each other with chosen amplitude and frequency so as to shear the sample. By measuring the force experienced by the plates one can estimate the viscous and elastic components of the material as a function of amplitude of the strain and shear rate. While bulk rheology is widely employed in industrial settings, protein condensates are not amenable to this technique because they (i) typically

appear in droplets within other fluids and (ii) they are often difficult to produce at milliliters scale.

One popular choice to measure the viscoelasticity of scarce samples is active or passive "microrheology",[80] a method that employs spherical particles embedded in the fluid of interest to probe its material properties. In the last 10−20 years, microrheology has been extensively used to characterize cellular structures in vitro as well as in vivo such as the cytoplasm, cytoskeleton, nucleoplasm, etc.[81−83] Microrheology can be done in passive or active mode. Passive microrheology leverages the thermal diffusion of particles within the fluid to extract information on its material properties.[82] A limitation of this technique is that it can only probe small deformations of the sample, driven by thermal noise alone. On the other hand, active microrheology employs optical tweezers to apply larger-than-thermal forces on the beads embedded in the fluid and measures the response of the fluid.[69,84] Note that there are techniques sitting in between the two and that use optical tweezers to trap the particles in place and study their thermal fluctuations.[85,86]

Using microrheology, Jawerth et al.,[13,69] Alshareedah et al.,[14] and Ghosh et al.[15] reported the most quantitative studies on the viscoelasticity of condensates in vitro so far. Jawerth and coauthors studied protein droplets formed by PGL-3 and proteins of the FUS family (FUS, EWSR1, DAZAP1, and TAF15) and found that these condensates behaved as "ageing" Maxwell fluids, i.e. as fluids displaying a frequency-dependent viscoelastic response with a relaxation time scale that became longer over time (see below). An intriguing discovery of their work is that the elastic plateau, i.e., the measure of elastic solid-like response of the condensate, does not appear to increase over time in aging droplets: older condensates are not harder than their younger counterparts. At the same time, this aging, or maturation, behavior was found to increase the intrinsic relaxation time of the fluid over time. This may reflect an internal rearrangement dynamics of the protein condensate; the macromolecular components reorganize to find deeper energy minima within the large configurational space in turn increasing the time scales of elastic response of the condensate. As pointed out in ref 13, this mechanism is not dissimilar to the physics of certain glasses, and from a biological standpoint, this aging process may eventually lead to pathological and irreversible condensates akin to amyloid fibrils. At the same time, Alshareedah et al.[14] performed passive microrheology on optically trapped beads (see below) and discovered that sequence composition of short polypeptides has a marked impact on the material properties of protein−RNA condensates. For example, they find that the condensates behave as Maxwell fluids and that polypeptides with sequences [RGXGG]$_5$ with X = [P, S, R, F, Y] display increasing values of viscosity from ∼0.1 to ∼40 Pa s. They also find that the relaxation time τ_R determining the time scale of elastic response varies from 0 (for P, S residues) to 1 s for [RGYGG]$_5$ for which the elastic plateau reaches up to 60 Pa. They also find that the presence and sequence of RNA has an effect on the condensate material properties and that the viscoelastic behavior is correlated with the strength of protein−nucleic acids interactions. Finally, Ghosh et al.[15] used active micro-rheology (see below) to show that heterotypic protein condensates form viscoelastic fluids and that the time scales of fusion in coalescence experiments (see below) is governed by the elastic component of the condensate. These studies highlight the impact that single residue mutations can have on
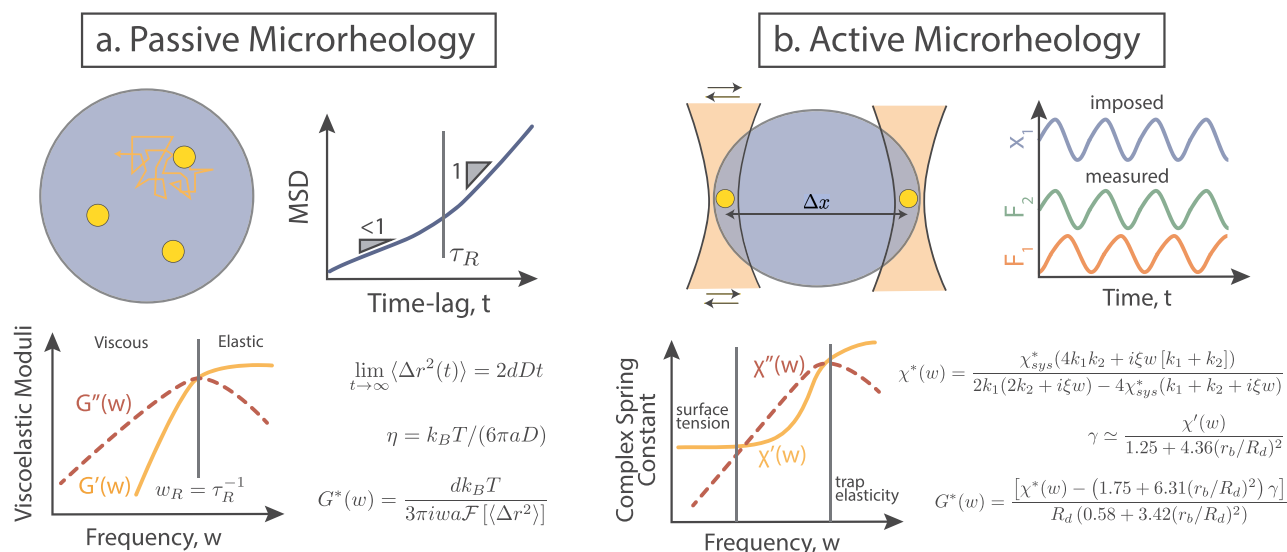
Figure 3. Microrheology of condensates. (a) Passive microrheology is performed by tracking the position of probe particles within a condensate. From the mean squared displacement, $\langle \Delta r^2(t) \rangle$, one can obtain the elastic and viscous moduli G', G'' which in turn quantify the full viscoelastic spectrum of the condensate and its viscous and elastic components as a function of deformation frequency. (b) Active microrheology is performed by trapping beads within a condensate and using them as "handles" to apply an oscillatory stress to the droplet. The complex and frequency dependent spring constant of the droplet can be computed by measuring the distance of, and forces experienced by, the particles as a function of the frequency of oscillations.

the behavior of the condensates and the ability of microrheology to provide quantitative and precise information on the flow properties of condensates. We thus now describe how to perform and critically interpret passive and active microrheology techniques in detail.

Passive Microrheology. In a typical passive microrheology experiment, a brightfield or epifluoresce microscope is used to record movies of passive spherical particles (typically around 0.1−1 μm in size) diffusing within the condensate. From these movies, particle tracking algorithms (such as TrackPy[87] or TrackMate[88] in ImageJ) are used to obtain the trajectories of the particles, $r(\tau)$ (Figure 3a). In turn, the mean squared displacement (MSD) for a given (lag-)time t is computed from the trajectories as

$$\langle \Delta r^2(t) \rangle = \langle [r(\tau + t) - r(\tau)]^2 \rangle \tag{1}$$

where the average is intended over particles and times τ. In other words, the mean squared displacement measures the (square) length explored by a particle in between any two points of its trajectory within a given time window t. For example, a "fast" particle may cover 1 μm^2 in $t = 1$ s, while a "slow" one may explore 0.01 μm^2 in the same $t = 1$ s. If we assume that the sample around the particle is at steady state, we expect that the particle mobility will not change in time during the observation. This implies that we expect the particle to have the same mobility in the first and last seconds of its trajectory, and for this reason, we can take the average over initial times τ in eq 1. In turn, the MSD is thus only a function of *lag-time t*. Importantly, for aging systems, such as FUS or PGL-3 droplets,[13] one should take care that the temporal average is shorter than the time scales over which the fluid changes its material properties to avoid confounding effects due to the particle mobility changing over the observational time scale.

In a viscoelastic fluid, being a condensate or not, the behavior of the MSD at *large enough times and unconfined space* is described by $\lim_{t \to \infty} \langle \Delta r^2(t) \rangle = 2dDt$, i.e., a freely diffusive behavior with diffusion coefficient D and $d = 1, 2,$ or 3 being the dimensionality of the tracked trajectory $r(\tau)$. For passive spherical tracers, the Stokes−Einstein relation connects the diffusion coefficient of the tracers D to the viscosity of the surrounding fluid η as

$$\eta = \frac{k_B T}{6\pi D a} \tag{2}$$

with a being the radius of the tracer, k_B the Boltzmann constant and T the system temperature. In some experimental conditions, and especially *in vivo*, it may not be possible to track the tracer beads for long enough times to observe their freely diffusive behavior, for instance, because of droplet movements that cannot be corrected or because the tracers sediment to the bottom of the sample. In these cases, one has to rely on measurements at shorter time scales, where the MSD may assume a more generic functional form

$$\text{MSD}(t) = K t^\alpha \tag{3}$$

where α is the exponent that describes whether the motion is constrained (also called subdiffusive, $\alpha < 1$) or active (also called superdiffusive, $\alpha > 1$). Importantly K is not a diffusion constant but rather a generic transport coefficient with units of length^2/time$^\alpha$ and if $\alpha < 1$ it cannot be used to extract the viscosity of a fluid via the Stokes−Einstein equation. In fact, in this case eq 2 would not even have the correct units of viscosity.

The conceptual leap to connect the tracers' trajectories to the frequency-dependent material properties of the condensate is done by realizing[80] that the MSD in the time-domain is connected to the so-called complex modulus in the frequency-domain $G^*(w)$ via a unilateral Fourier transform (or a Laplace

transform followed by an analytic continuation) also known as a Generalized Stokes−Einstein Relation (GSER)[80,89]

$$G^*(w) = G'(w) + iG''(w) = \frac{dk_B T}{3\pi i a w \mathcal{F}[\langle \Delta r^2(t) \rangle]} \quad (4)$$

where $d = 1$, 2, or 3 is the dimension of the position vector used to compute the MSD and $\mathcal{F}[\cdot]$ indicates the unilateral Fourier transform. The complex modulus G^* is a powerful function that describes the material properties of the complex fluid in the frequency or time domains. From the complex modulus, the elastic and viscous moduli G' and G'', respectively, can be obtained as the imaginary and real parts of G^*. These frequency-dependent functions encode the propensity of the complex fluid to react like a viscous fluid or as an elastic solid to a linear deformation with frequency w. One of the simplest models of viscoelastic fluids is the so-called Maxwell fluid, which displays a crossover frequency w_R at which the fluid switches from viscous to elastic behavior (see Figure 3a). For frequencies $w < w_R$, i.e., time scales $t > \tau_R = w_R^{-1}$, the material flows like a liquid and this is reflected by the fact that $G'' > G'$; on the contrary, at frequencies $w > w_R$, or time scales $t < \tau_R$, fast deformations trigger an elastic response, i.e., $G'' < G'$.

In the context of microrheology, it is also worth mentioning the importance of accurately measuring the "noise floor".[90] Indeed, the noise from experimental conditions, equipment, etc. will affect the precision at which particles are tracked and will in fact appear as a non-zero plateau in the MSD curves at early times. In turn, this will be transformed by the GSER into an elastic contribution of $G'(w)$ at large frequencies. Thus, the noise must be assessed by measuring the MSD of beads immobilized on the coverslip and under the same experimental conditions as the other tracers. Failing to do so may yield an incorrect interpretation of the results and an overestimation of the elasticity of the condensate.

We note that passive microrheology stands out from other techniques as it is minimally invasive. For instance, bulk rheology shears the sample by pressing on it, in turn inducing some stiffening.[91] At the same time, it can only probe small deformations of the fluid as the motion of the beads is thermally driven. Arguably, the forces experienced by condensates *in vivo* may be larger than thermal ones, and in the next section we discuss how these "nonlinear" regimes may be explored.

Finally, we mention that particle tracking is not the only way to obtain MSD curves from the recording of particles diffusing in a system. In fact, one can also employ Differential Dynamic Microscopy (DDM), a technique that relies on the spatial and temporal autocorrelation of the pixel intensities in order to extract the dynamics of the particles in the system.[92−94] This technique is particularly well suited for particles that are too small to be resolved with optical microscopy or to measure the dynamics of fluorescently labeled probes and molecules, such as small DNA plasmids.[95]

Optical Trap Microrheology. In microrheology, the longer the particles are imaged the better the average and the broader the spectrum of frequencies that can be sampled. Yet, in some experimental conditions it may be difficult to image the particle for long times because of sedimentation or other experimental challenges. For this reason it may be more appropriate to trap the particles using an optical tweezer and measure their thermally induced displacements.[14,15] The

optical tweezer effectively traps the particle in a harmonic potential with certain stiffness that should be calibrated and that can be tuned by setting the laser power. Because of the trap, the particle is not allowed to escape and freely diffuse in the sample. Its diffusion is thus constrained at large times, and the (squared) displacements will display a plateau that is related to the trap stiffness κ as $\langle r^2 \rangle = 3 k_B T/\kappa$ where $\langle r^2 \rangle$ is the time-independent variance of the displacement vector $r(t)$ or, in other words, is the value of the MSD at infinite time. Using the *normalized* mean squared displacement (NMSD) $\langle \Delta r^2(t) \rangle_n \equiv \langle \Delta r^2(t) \rangle/2 \langle r^2 \rangle$ one can obtain the complex modulus as[85]

$$G^*(w) = G'(w) + iG''(w) = \frac{\kappa}{6\pi a} \left(\frac{1 - iw\langle \Delta \tilde{r}^2(w) \rangle_n}{iw\langle \Delta \tilde{r}^2(w) \rangle_n} \right) \quad (5)$$

where $\langle \Delta r^2(w) \rangle_n$ is the Fourier transform of the NMSD. Several postprocessing, oversampling, and optimization protocols have been developed for this technique, and it can give up to 5−6 decades of viscoelastic spectrum with a single measure.[85,86]

Active Microrheology. Active microrheology, where a bead is trapped and moved around the sample by an optical trap, is widely employed to probe the so-called "nonlinear" response of a system to larger-than-thermal forces.[84,96] Additionally, this technique is appropriate for systems that are simply too stiff to be studied by thermal fluctuations only and in which the passive tracers hardly move at all. Recently, a novel active microrheology technique has been developed to extract the complex moduli and surface tension from protein droplets. The technique relies on two beads embedded in a condensate and trapped by two independent optical tweezers. One of the tweezers is kept static while the other is made to move, thereby creating an oscillatory stress on the sample[15,69] (Figure 3b). During the experiment, the forces acting on both beads are measured and used to determine the frequency-dependent effective spring constant of the whole system (droplet and traps) as

$$\chi_s^*(w) = \frac{\tilde{F}_2 - \tilde{F}_1}{2\Delta \tilde{x}} \quad (6)$$

where $\tilde{F}_i$ is the Fourier transform of the force on bead i and $\Delta \tilde{x}$ is the Fourier transform of the relative position of the beads $\Delta x(t)$. One can then derive the complex spring constant, encoding only the viscoelasticity of the droplet as[69]

$$\chi^*(w) = \chi'(w) + i\chi''(w)$$
$$= \frac{\chi_s^*[4k_1 k_2 + i\xi w(k_1 + k_2)]}{2k_1(2k_2 + i\xi w) - 4\chi_s^*(k_1 + k_2 + i\xi w)} \quad (7)$$

From this equation, it is possible to extract two contributions: first, the surface tension, which dominates at slow deformations, i.e., small w, as

$$\gamma \approx \frac{\chi'(w)}{1.25 + 4.36(r_b/R_d)^2} \quad (8)$$

which is valid in the limit that the bead is small compared with the droplet ($r_b \ll R_d$) and, second, the full complex modulus as

$$G^*(w) \approx \frac{[\chi^*(w) - (1.75 + 6.13(r_b/R_d)^2)]\gamma}{R_d(0.58 + 3.42(r_b/R_d)^2)} \quad (9)$$

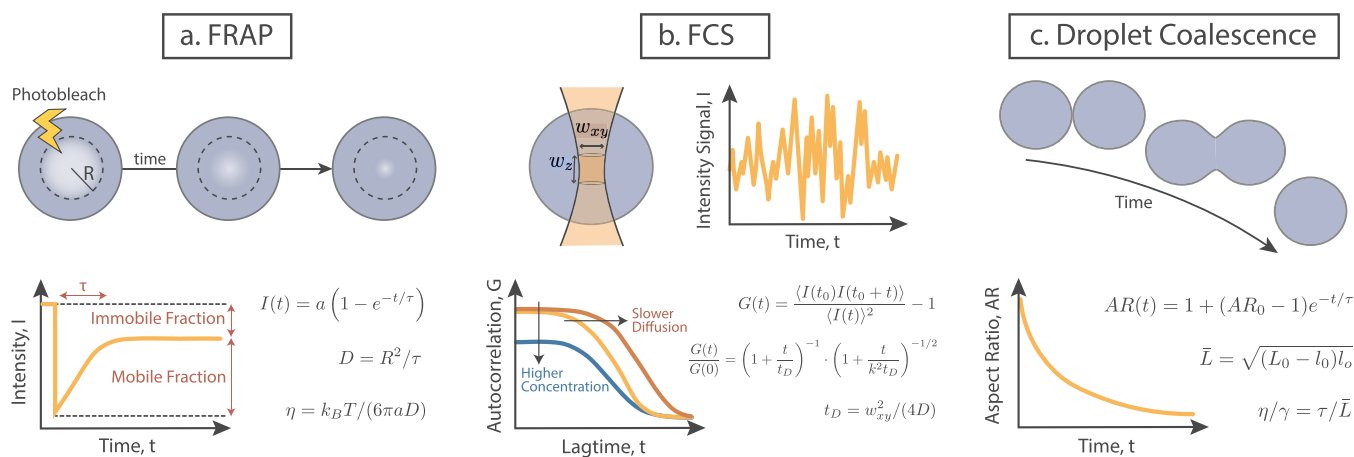which is again valid if $r_b \ll R_d$ and if $|G^*(w)|R_d \gg \gamma$.

Figure 4. Fluorescence-based methods to characterize viscosity and surface tension of condensates. (a) FRAP is performed by bleaching a region (disk, strip, whole) of the condensate. The FRAP recovery curves are typically fitted by a single expoenential function which returns a single characteristic time scale of protein rearrangement within the droplet. This time scale can be translated into an apparent diffusion coefficient of the proteins $D = R^2/\tau$ (see ref 39) which in turn may be used to crudely estimate the apparent viscosity η via the Stokes−Einstein relation.[5] (b) FCS is performed by detecting fluorescent molecules (typically GFP or proteins) diffusing through a small (∼femtoliter) volume within the sample. After fitting the autocorrelation function $G(t)$ the apparent diffusion constant is obtained as $D = w_{xy}^2/(4\tau)$, where w is the size of the sampled volume. A big advantage of FCS over FRAP is that it can quantitatively measure the concentration of molecules in the illuminated volume. (c) Passive droplet coalescence can quantify the relaxation time scale of droplets. Assuming pure Newtonian behavior, the balance of viscosity and surface tension determines the typical relaxation time scale as $\tau = \eta/\gamma L$. Active droplet coalescence, done by pushing together droplets trapped by optical tweezers, can overcome some technical problems of passive coalescence experiments.

While this is a useful and quantitative technique, it requires a microscopy set up with two independent and finely calibrated optical tweezers, which is not common in molecular biology laboratories. It also requires the production of large droplets (∼10−20 μm) and spherical particles with large refractive index that can be trapped inside the condensate. Additionally, while it can yield both the surface tension and the viscoelastic spectrum in one measurement, the range of usable frequencies for $G^*(w)$ is relatively small, given the fact that the small ($w \lesssim 0.1$ s^{-1}) and large ($w \gtrsim 10$ s^{-1}) regimes are dominated by surface tension and trap stiffness

Overall, we find that passive and active microrheology are currently the best techniques to quantify in full the viscous and elastic properties of condensates. Indeed, other techniques such as FRAP and FCS (see below) cannot yield a full viscoelastic spectrum of the condensate. In spite of this, microrheology is not a common technique in biology (yet): active microrheology would be very challenging to perform *in vivo*; on the other hand passive microrheology has been performed *in vivo*[82] but requires microinjection to be performed in the nucleus.[73,83] Below, we thus describe more widely employed techniques in biology which can also give information on the condensates material properties albeit not as complete as microrheology.

Finally, we note that it is possible to measure viscosity and surface tension of *in vitro* condensates bypassing microscopy or optical tweezers by using "micropipette aspiration".[76]

Fluorescence-Based Techniques

Fluorescence Recovery after Photobleaching. Fluorescence Recovery After Photobleaching (FRAP) is a popular technique to study the dynamics of cell components and has now been extensively employed to measure the dynamics of cellular phase condensates. FRAP requires fluorescently tagged proteins or molecules and strong lasers and is thus typically performed on a confocal microscope. It works by permanently inactivating ("bleaching") some of the fluorescent probes in

the sample within a region of the cell or droplet, which could be a disk of radius R, a strip, or a larger region (see Figure 4a). After the bleaching step, the intensity of the fluorescence signal within the bleached region (and that in a control region) are monitored over time. Hence, this technique probes the dynamical rearrangements of the macromolecular components of the cell or droplet either within the droplet or with the soluble pool. Typical FRAP curves display a sudden drop (the bleaching step) followed by a recovery of the normalized intensity signal. This recovery mirrors the diffusion, binding and reaction activity of the fluorescently labeled molecules or proteins within the sample; a process that can be modeled as a system of differential reaction/diffusion/advection equations with single or multiple binding states.[97−99] It has been noted that depending on the model used to fit these curves the values obtained for the on and off binding rates of certain transcription factors can vary widely.[99,100] The analysis and interpretation of these curves is thus a critical step. In the absence of an *a priori* hypothesis on which model to use, the most agnostic way to extract information from FRAP curves is to numerically estimate the half time (time at which the signal has recovered half of its original value) and the intensity of the long time plateau.[101] Alternatively, for simple reaction processes one may also fit these FRAP recovery curves with a function of the form[101]

$$I(t) = a(1 - e^{-t/\tau}) \tag{10}$$

where τ is the mean recovery time and a the fraction of mobile proteins, i.e., the part of the signal that is recovered at infinitely large times (see Figure 4a). The mean recovery time τ is a characteristic time of reorganization within the cell or droplet for the fluorescently tagged protein. From it, one can extract a characteristic diffusion coefficient as $D = R^2/\tau$, with R the size of the bleached region, and in turn obtain an apparent viscosity from the Stokes−Einstein equation $\eta = k_{\mathrm{B}}T/(6\pi aD)$, where a is here the expected radius of the protein of interest (see Figure

4a). This reasoning assumes that the droplet is a simple Newtonian fluid and cannot distinguish binding and diffusion of the protein of interest. For instance, if the recovery time is very long, it cannot dissect if the reason is because the protein has long binding times or slow diffusion. Albeit crude, this approach has been extensively used in the literature to estimate the viscosity of protein droplets. For instance, by performing FRAP on large *C. elegans* P granules *in vivo*, their viscosity was estimated to be[5] $\simeq$1 Pa s, which was broadly consistent with the viscosity measured via microrheology on the P granules component LAF-1 *in vitro* and in the presence of RNA.[102]

Another piece of information that can be extracted from FRAP curves without making any *a priori* hypothesis on the dynamics and binding modes of the protein of interest is the large time recovered fraction. In eq 10, the coefficient *a* represents the recovered fraction of the signal while its counterpart 1-*a* is the fraction of signal that has not recovered. This is typically referred to as the "immobile" fraction and reflects an intrinsic solid-like behavior of the protein of interest in the bleached region. For this reason, measuring the mobile and immobile fractions can qualitatively establish the liquid or solid nature of the droplets. For instance, incomplete FRAP recovery was interpreted as a qualitative indication of viscoelasticity of fibrillarin droplets.[4]

FRAP is widely employed because it is a technically straightforward technique that can be performed with a confocal microscope and yields a quick readout. If the scope is to extract qualitative information on the sample, then FRAP does not require complex postprocessing analysis and eq 10 can be used to fit the curves.[101] On the other hand, if the scope is to extract quantitative and precise information on binding and diffusion modes of proteins, then FRAP requires more complicated analysis and fitting models.[99]

An additional advantage of FRAP is that it is suitable *in vivo* as it only requires that cells express a fluorescently labeled protein. A potential shortcoming in this respect is that overexpressing a protein *in vivo* may saturate its binding sites or compete with the endogenous protein species in turn generating confounding results when compared with knock-ins or single-particle tracking.[100] At the same time, the fluorescent tags that are typically used are, in some cases, as big as the proteins themselves thereby affecting their native state and dynamics. For example, while it is common practice to fuse a GFP tag on the protein of interest, this may itself interfere with the correct protein function. Other less invasive labeling methods may thus be preferred.[103] Additionally, proteins are typically smaller than the pore size of the surrounding mesh, and hence, their apparent diffusion coefficient likely underestimates the bulk viscosity of the system.[70]

Another important source of potential confusion in the FRAP results is that in heterotypic condensates recovery curves may be widely different depending on which population of proteins is considered as fluorescent probes. This is due to the fact that different proteins and/or nucleic acids in a condensate may display different structural roles with shorter/longer relaxation times. For instance, condensates of HP1α with DNA fragments display recovery curves that are slower for longer DNA fragments if DNA is used as the fluorescent probe; on the contrary, no change in recovery time is observed if the fluorescently labeled probe is HP1α.[104] Similar results were seen in DNA condensates mediated by crowders or H1.[105] This indicates that these condensates are viscoelastic, with the DNA providing the elastic contribution. These observations

can be well explained by the "bridging induced phase separation" (BIPS) model, explained below. Hence, in the case of heterotypic condensates fast dynamics of one of the components may be erroneously interpreted as indicating a purely liquid droplet and FRAP should thus be performed on all the components of a condensate to estimate its bulk viscoelastic nature.

Fluorescence Correlation Spectroscopy. A popular high-resolution technique that is even more powerful than FRAP is Fluorescence Correlation Spectroscopy (FCS). It employs a confocal microscope to illuminate an approximately femtoliter volume in the sample (see Figure 4b). Fluorescently tagged proteins travel through the illuminated volume, and fast detectors are used to record the variation in the intensity of the signal. The time trace of the signal is acquired and autocorrelated as[106]

$$G(t) = \frac{\langle I(t_0)I(t_0 + t) \rangle}{\langle I(t) \rangle^2} - 1 \tag{11}$$

where the average is intended over times t_0 and the -1 is there to ensure that $G(\infty) = 0$. Even neglecting submicrosecond correlations (not relevant for this review), the analysis and fitting of FCS autocorrelation curves can be as complicated as the ones for FRAP curves. Different fitting models with multicomponent diffusion, advection and reaction kinetics have been proposed.[107−109] In the simplest scenario, with one diffusing component, the autocorrelation curve takes the functional form

$$G(t) = G(0)\left(1 + \frac{t}{t_D}\right)^{-1}\left(1 + \frac{t}{k^2 t_D}\right)^{-1/2} \tag{12}$$

where $G(0) = \pi^{3/2} w_{xy}^2 w_z / c$ is related to the average concentration of probes c in the illuminated volume of sizes w_{xy} and w_z (k is the ratio $k = w_z/w_{xy}$) and $t_D = w_{xy}^2/(4D)$ is the time it takes for a probe to diffuse through the illuminated volume. This fitting model with a single diffusing component was used to extract the relaxation time t_D (and hence apparent diffusion) of protein components in optogenetic droplets[110] but multiple diffusing populations can also be used if needed. As in the case of FRAP, the characteristic time scale of the protein diffusion can be translated into an apparent diffusion constant and, in turn, to an estimate of the solution viscosity, provided that the small size of protein probe is acknowledged.[35,110−113] The big advantage of using FCS over FRAP is that, beyond measuring protein dynamics, it can also measure protein concentration which is extremely useful in order to compile a quantitative phase diagram of the phase-separated system.[35,110]

We mention that while performing nonconventional FCS methods such as multiscale FCS[70] and raster image correlation spectroscopy[114] can give effective mean squared displacements of the probes by measuring spatial and temporal intensity fluctuations (akin to differential dynamic microscopy[92]), they cannot be translated into the complex modulus $G^*(w)$ via the generalized Stokes−Einstein relation (eq 4) because such equation assumes that the probes are bigger than the pore size of the surrounding fluid.[80] On the contrary, GFP molecules and fluorescently tagged proteins are typically smaller than pore or mesh size of their surrounding environment. For instance, compare the ~10−100 nm for chromatin[70,79] with the typical size of GFP ~ 5 nm. In turn, this implies that the

MSDs obtained from FCS give information on the "nano-rheology" of the system and are likely to underestimate the mesoscale viscosity and elasticity of the bulk.

We finally mention that alongside FRAP and FCS, single particle tracking using, for example, photoconvertible dyes and/or super-resolution techniques are becoming widely employed and precious tools to obtain high-resolution information on the dynamics of proteins in these condensates.[115−120] This is particularly the case *in vivo*, as placing other types of probes is far more challenging. Importantly, since these tracked proteins are typically actively interacting with the surrounding, they cannot be used as a proxy for microrheology to extract the viscoelasticity of the sample via the GSER. Indeed, GSER assumes that the probes are passive and do not interact with the environment.

Droplet Coalescence. In droplet coalescence assays, condensates are imaged in fluorescence or brightfield mode and fusion events recorded. When two droplets meet they will, if liquid-like, form a neck between them, in turn transforming into an elongated shape that will eventually relax to a round drop due to surface tension (see Figure 4c). The higher the surface tension, the faster an elongated droplet will relax to a spherical shape; this relaxation is opposed by viscosity which will in fact resist against the reshaping and increase the overall relaxation time. The evolving condensate is imaged at fast temporal resolution and its major and minor axis extracted via fitting of an oval shape or an asymmetric Gaussian. The ratio of minor (l) and major (L) axis yields the droplet aspect ratio AR which typically displays a simple exponential decay from the value of two round droplets stuck to each other to that of a single round droplet (see Figure 4c)

$$\text{AR}(t) = \frac{L(t)}{l(t)} = 1 + (\text{AR}_0)e^{-t/\tau} \tag{13}$$

where τ is the relaxation time and it is proportional to characteristic droplet size $= L$ (often taken as the average of droplets' diameters at $t = 0$, i.e., $\overline{L} = \sqrt{(L_0 - l_0)l_0}$):

$$\tau = \frac{\gamma}{\eta}\overline{L} \tag{14}$$

By fitting the relaxation times obtained by tracking the evolution of the aspect ratio for droplets of different sizes one thus expects a straight line with slope η/γ, the so-called capillary velocity (the ratio between the viscosity η and the surface tension γ).[5,6,111] Similar to FRAP, this technique is straightforward and does not require heavy postprocessing. The downside is that it is not possible to extract the values of η and γ separately and other techniques should be coupled to it, e.g., microrheology.[102,111]

Interestingly, the coalescence of droplets is one of two mechanisms expected for the growth of liquid condensates. Alongside coalescence due to fusion of neighboring droplets, the so-called "Ostwald ripening" process predicts that smaller droplets should shrink to the benefit of the growth of bigger ones due to energy minimization and surface tension.[121−123] Both mechanisms predict that the typical size of the droplets should grow in time as $r \sim t^{1/3}$.[121] On the other hand, it was recently found that *in vivo* there is (i) no evidence of Ostwald ripening and (ii) the growth of nuclear droplets follows a scaling law $r(t) \sim t^{0.12}$ slower than that expected for either Ostwald ripening or coalescence.[124] These two unexpected observations were explained considering that *in vivo* nuclear condensates grow in a viscoelastic medium, i.e., the chromatin, which is more akin to a melt of polymers[125] than to a purely viscous fluid. The behavior of liquid−liquid phase separation within viscoelastic environments is rather unexplored and only recently started to be addressed in *in vitro* experiments[126,127] and theory.[122]

Finally, it is worth noting that experiments measuring passive droplet coalescence have a number of potential pitfalls. They may be affected by the surface onto which the droplets sit and diffuse; e.g., if the surface is not perfectly hydrophobic, it will create an effective friction that will slow down the fusion dynamics. It also relies on stochastic events and, thus, is typically inefficient and time-consuming. Finally, for droplets with large surface tension, the fusion event may be very fast, thereby rendering the analysis challenging. To circumvent these problems, droplets were recently forced to fuse by using optical tweezers.[111,128−131] This technique removes surface effects because the droplets are trapped in the bulk before sedimentation and it provides a finer control over the time scales of fusion and number of events recorded.[111] The analysis is typically done on the recorded laser signal and considering an exponential relaxation process (droplet relaxation) coupled to the linear movement (constant speed) of the trap across the droplet as follows[132]

$$S(t) = ae^{-t/\tau} + bt + c \tag{15}$$

where a, b, c, and τ are fitting parameters.

It should be noted that the analysis of the passive and active droplet coalescence described above assumes Newtonian droplets which display a single relaxation time scale associated with their viscosity and surface tension (see eq 14). In the case of viscoelastic droplets the analysis is less straightforward because the droplets may themselves display one, or multiple, relaxation time scales associated with the transition from elastic to viscous behavior.[14,15,131] For instance, homotypic viscoelastic droplets pushed together by optical traps are not expected to be able to fuse until after the internal relaxation time scale,[15] and in this sense their apparent viscosity measured using the Newtonian approximation should yield much higher values than the real one. At the same time, heterotypic droplets made of different polymers would require specific experimental conditions (e.g., temperature, pH, osmolarity) to favor miscibility (mixing) of the polymer species. From the Flory−Huggins theory, the longer the polymers the lower the critical Flory parameter needed to trigger phase separation in heterotypic polymer solutions as $\chi_c \sim 1/N$, with N the length of the polymers.[16] When outside the miscibility region, heterotypic droplets are still seen to display a range of arrangements (wetting, partial engulfment, or complete engulfment) depending on the relative surface tensions.[4,128]

Finally, we mention that droplet fusion has been extensively used in the literature as evidence of the liquid nature of the protein condensates. Passive droplet coalescence is, in fact, particularly suited *in vivo* as it can be visualized with standard fluorescence or confocal microscopes,[19] although tracking the aspect ratio of submicron size droplets in vivo is very challenging.[64,75] On the contrary, active droplet coalescence has only been done *in vitro* as it requires a significant difference in refractive index between the inside and outside of the droplets in order to trap them.

Models of Phase Separation

Currently, liquid−liquid phase separation (LLPS) is the most invoked mechanism to explain the appearance of membrane-less droplets. In spite of this, recent works cast some doubts on the validity of LLPS to explain some experimental observations,[133,134] such as the wide difference in the FRAP recovery for different components of heterotypic condensates[104] or the unrestricted diffusion of PolII across replication compartments.[115] An alternative model to LLPS that may explain these findings is the so-called "bridging induced attraction" or "bridging induced phase separation" (BIPS) model[23,24,135,136] (also referred to as "polymer−polymer phase separation" in some works[137]).

BIPS is a demixing process qualitatively different from LLPS in that it requires (i) a long polymeric substrate and (ii) proteins with two or more binding sites, i.e., multivalent. As we describe in detail in this section, BIPS ultimately yields condensates reminiscent of associating polymers which are well-known to display viscoelastic behaviors.[138] Typical examples of BIPS are the condensation *in vitro* of DNA with HP1,[104] H1,[105] and yeast cohesin.[23] Because of the multivalent binding (or effective multivalent binding due to di/oligo-merisation), these proteins are able to form loops on the polymer and locally increase the concentration of available binding sites. The nucleation of such a polymer loop triggers a positive feedback, as a locally larger concentration of binding sites will attract more proteins, which will in turn form more loops and themselves increase the density of polymer segments, or binding sites. Additionally, there is an entropic push to cluster proteins together, therefore creating fewer distinct loops within the same polymer.[24,135,136] This entropic clustering mechanism was first proposed in ref 24. BIPS ultimately drives the coarsening and coalescence of clusters of proteins interwoven within the polymer (DNA or chromatin) substrate.[24,135] Importantly, these protein clusters—which would not exist without the polymeric substrate—appear to have surface tension and to grow as expected for classic Ostwald ripening and coalescence of demixing liquid droplets but could also be arrested by introducing nonequilibrium binding modes[135,139] or by limiting their binding to specific DNA sites.[24,140] Simulated FRAP on BIPS-driven protein clusters show that they can recover by exchanging with the soluble pool while the underlying polymeric framework is glassy and evolves on much longer time scales,[135] in line with what observed in FRAP experiments of HP1α and DNA droplets.[104] BIPS also predicts that FRAP recovery curves for the polymer itself would depend on its length, as the longer the polymer the more entangled and the slower to rearrange,[135] consistent with the observations in ref 105.

BIPS can also explain the recent observation of enrichment of PolII into viral replication compartments (RC) in Herpex Simplex infected cells.[115] Here, BIPS is triggered by the fact that the viral genome is enriched in highly accessible (ATAC) sites, and so it displays a large number of nonspecific binding sites for PolII in turn triggering the feedback loop described above. This is consistent with the single molecule tracking data suggesting weak transient binding events of PolII inside the RC.[115] A similar argument explains the unrestricted motion of PolII in and out of RC due to the abundance of nonspecific binding sites inside the RC. Furthermore, in general, BIPS-driven droplets are far less sensitive on the concentration of the protein component: in LLPS, a certain critical concentration must be attained before triggering demixing. Increasing the

concentration of protein past this critical concentration will not change the concentration within the dense phase, only its volume. This is not the case in BIPS, which can be triggered at very low protein concentrations and can increase the concentration of the dense phase as long as it displays free binding sites. Another peculiar feature of BIPS is that the polymer is compacted by the presence of the proteins, yet this process does not necessarily produce a dense and inaccessible polymer globule; on the contrary, the degree of polymer compaction depends on the number of binding sites in the protein of interest; for instance, yeast cohesin was found to maintain a rather open DNA structure compatible with bivalent binding.[23]

How can we distinguish LLPS from BIPS using the methods described above? First, due to the presence of a long polymeric substrate, BIPS-driven condensates are typically viscoelastic and reminiscent of systems of associating polymers, yet their protein component may display fast exchange within the condensate and with the soluble pool, as in the case of DNA and HP1α condensates.[104] Thus, microrheology with large probes, FRAP on the polymeric component, and droplet coalescence have the best chances to reveal the elastic contribution to the droplet material properties. At the same time, while LLPS-driven droplets can be either viscous or viscoelastic, BIPS-driven droplets cannot be purely viscous because triggered by a long (typically entangled) polymer substrate. Similarly, active microrheology and active/passive droplet coalescence should reveal their sluggishness due to the intrinsically slow polymer network, which can be thought of as a transiently cross-linked polymer gel. The intrinsic relaxation time of the droplet is thus related to the time scales of the cross-links, i.e., protein on/off kinetics[135] and stoichiome-try,[21,141] and entanglements, related to the length of the polymer.[142] In line with this, in refs 104 and 105, droplets made with longer DNA presented more irregular and nonspherical shapes with DNA-length dependent FRAP recovery. To the best of our knowledge, no microrheology was performed on those droplets but we expect them to display a strong elastic component that grows with the length of the polymer substrate.

Distinguishing LLPS from BIPS *in vivo* is more challenging as microrheology cannot be easily performed in the cell nucleus. For a protein known or suspected to bind DNA/chromatin, then FRAP or FCS should be performed on both the protein and the underlying DNA/chromatin component (or on fluorescently labeled histones as a proxy for chromatin). Additionally, since BIPS cannot be triggered without a long polymeric substrate, purifying the protein of interest and testing its tendency to phase separate in presence of long DNA *in vitro*, e.g., using commercially available lambda-DNA, is potentially one the best way to test LLPS versus BIPS.

We note that LLPS and BIPS are not the only two models that have been proposed to explain the behavior of intrinsically disordered proteins. Indeed, the "phase-separation-aided bond percolation" (PSBP) model[22] is an appealing model for condensates made of multivalent proteins. It connects the condensate material properties to critical percolation phenom-ena in systems of associating polymers and is particularly appropriate to explain aging and hardening of condensates, as seen in ref 13. PSBP differs from LLPS as it introduces complexity in the form of long-lived bridging between proteins and so it requires direct protein-protein attraction to be triggered. PSBP also differs from BIPS in that the latter does

not require direct protein−protein attraction but it requires a long polymer substrate (such as long DNA or RNA segments) and multivalent DNA/RNA binding proteins to initiate and form condensates. For instance, in ref 23 it was shown that yeast cohesin did not form clusters, unless in the presence of a long enough DNA molecule. In general, in BIPS the viscoelastic nature of the condensates largely relies on the entanglement and transient cross-linking of the long scaffold. Note that LLPS may, in some cases, act as a precursor of PSBP, and we therefore stress that the most glaring difference between LLPS/PSBP and BIPS is that the latter requires an underlying polymer scaffold to which proteins bind to.

We argue that, as often is the case in biology, multiple mechanisms may be at play and may be in place to address different biological requirements. For instance, while liquid condensates may accelerate reactions, viscoeleastic conden- sates may offer transient structural support.[29] In line with this, the use of terminology such as LLPS should be avoided unless supported by appropriate evidence[134]; indeed, it may conceal biophysical properties which could be relevant for the condensate's physiological functions. For this reason, other mechanisms such as BIPS and PSBP, and the condensates material properties, should be considered and appropriately examined.

■ DISCUSSION AND CONCLUSIONS

While some may argue that protein condensation in biology is "just a phase", we feel that this field is putting the spotlight on previously underappreciated universal mechanisms that are employed by life to sense, respond, organize, and control intracellular processes. Generic physical principles such as phase separation and demixing which were traditionally studied by physicists, chemists and engineers to describe metal alloys and binary fluids[16,143] now find application to describe the behavior of proteins and nucleic acids inside living cells. This clearly creates a unique nexus and a meeting point between very different disciplines. In the near future this field will likely attract an even broader interdisciplinary audience.

The main point of this Perspective is that experiments performed in the past decade have uncovered that phase separation (LLPS or BIPS)—defined as thermodynamically driven, reversible demixing of liquid phases—can trigger the onset of non-Newtonian fluid behaviors, e.g., viscoelasticity, via the interaction of intrinsically disordered protein domains with themselves or with nucleic acids. Because of this, phase separation and viscoelasticity should in fact be thought of as two sides of the same coin. The observation that condensates are round and that they coalesce over long times is not unambiguous proof that they are simple viscous liquids. Additionally, even if they were simple liquids at early times, there is no guarantee *a priori* that they will always remain so.[13] Among the techniques we reviewed above, active and passive microrheology stand out, as they can provide quantitative information on the full viscoelastic spectrum of the condensates.[13–15,69] Microrheology will in fact be able to assess if a protein droplet is a simple liquid (no elastic modulus G') or if it displays elastic response to deformations and at which time scales they appear to be dominant over the viscous ones. In spite of this, microrheology is very challenging to perform *in vivo*, and it is not a familiar technique in biology (yet). More commonly employed techniques are FRAP, FCS, and droplet coalescence assays which can probe the viscosity and surface tension of the condensates but cannot quantify the

response of the droplets to deformations occurring at different frequencies. Additionally, FRAP and FCS are "nanorheology" techniques as they rely on small probes (GFP or fluorescent proteins) which are likely to underestimate the bulk viscosity of the sample and fail to detect its mesoscale elasticity.

It is also appropriate to mention here that the inside of the cell is a busy environment where many biomolecules are involved in energy-consuming processes. It should therefore not be a surprise if certain protein condensates were controlled by out-of-equilibrium processes, for instance, involving post- translational modifications,[67,119,139,144,145] reaction-diffusion networks,[146−148] or environment elasticity.[124,126,149] In these cases, it would be even more intuitive to expect unconventional flow properties associated with the nonequilibrium nature of the droplets.

While we refrain from discussing in detail the simulations of protein phase separation (see ref 150 for a comprehensive review), we mention that, currently, simulations are mainly concerned with capturing the demixing and phase behaviors rather than the viscoelastic properties of droplets.[21,151−153] The reason for this may be that protein condensation encompasses a broad range of time- and length-scales[9,32,154] which are difficult to capture within the same model. For instance, near atomistic models may be needed to capture the correct phase behavior, while more coarse grained models are necessary to model bulk viscoelasticity. Because of this, multiscale modeling of protein condensates and their viscoelastic properties is a field that is just beginning to appear and will likely attract a number of computational researchers from soft matter, rheology, polymer physics, and fluid mechanics.

The next steps in this quickly expanding field will certainly involve more research *in vivo*; the connection between the condensation of a certain protein *in vitro*—sometimes under extreme crowding or salt conditions—and its biological relevance is oftentimes weak or circumstantial. Alongside this, we feel that often condensates are misclassified as originating from liquid−liquid phase separation because too little is known about other potential mechanisms.[134] As discussed above, bridging-induced phase separation[23,24,135] is an appealing alternative mechanisms to explain a range of observations, such as viral replication compartments in Herpes simplex infected cells[115] or even Polycomb[67] and hetero- chromatin[140,155,156] compartments. We expect that in the DNA-rich eukaryotic nucleus this mechanism may well dominate over more traditional liquid−liquid phase separation.

Finally, we stress that the nontrivial flow behaviors of certain protein condensates may have important biological relevance. For instance, viscous droplets may provide a crucible to accelerate reactions or to slow them down by sequestering certain enzymes; on the other hand condensates with a (visco)elastic behavior may provide structural support to shape genome organization,[59,68] control chromatin dynamics,[141] and regulate enhancer−promoter interactions.[157] By using the methods and the concepts provided in this review, we thus hope that the research community will be better equipped to answer these outstanding questions.

■ AUTHOR INFORMATION

Corresponding Author

Davide Michieletto − *School of Physics and Astronomy, University of Edinburgh, Edinburgh EH9 3FD, U.K.; MRC*

Human Genetics Unit, Institute of Genetics and Cancer, University of Edinburgh, Edinburgh EH4 2XU, U.K.;
ⓘ orcid.org/0000-0003-2186-6869;
Email: davide.michieletto@ed.ac.uk

Author

Mattia Marenda − *School of Physics and Astronomy, University of Edinburgh, Edinburgh EH9 3FD, U.K.; MRC Human Genetics Unit, Institute of Genetics and Cancer, University of Edinburgh, Edinburgh EH4 2XU, U.K.;*
ⓘ orcid.org/0000-0001-5951-3212

Complete contact information is available at:
https://pubs.acs.org/10.1021/jacsau.2c00055

Notes

The authors declare no competing financial interest.

REFERENCES

(1) Alberts, B.; Johnson, A.; Lewis, J.; Morgan, D.; Raff, M. *Mol. Biol. Cell*; Taylor & Francis, 2014; p 1464.

(2) y Cajal, S. Unsencillo méthodo de coloracion dei reticulo protoplasmico e sus efectos en los diversos centros nerviosos de verte brados [ill] invertebrados. *Trab. del Lab. de investig. biol., Madrid* **1903**, *2*.

(3) Gall, J. G. The centennial of the Cajal body. *Nat. Rev. Mol. Cell Biol.* **2003**, *4*, 975−980.

(4) Feric, M.; Vaidya, N.; Harmon, T. S.; Mitrea, D. M.; Zhu, L.; Richardson, T. M.; Kriwacki, R. W.; Pappu, R. V.; Brangwynne, C. P. Coexisting Liquid Phases Underlie Nucleolar Subcompartments. *Cell* **2016**, *165*, 1686−1697.

(5) Brangwynne, C. P.; Eckmann, C. R.; Courson, D. S.; Rybarska, A.; Hoege, C.; Gharakhani, J.; Julicher, F.; Hyman, A. A.; Germline, P. Granules Are Liquid Droplets That Localize by Controlled Dissolution/Condensation. *Science* **2009**, *324*, 1729−1732.

(6) Brangwynne, C. P.; Mitchison, T. J.; Hyman, A. A. Active liquid-like behavior of nucleoli determines their size and shape in Xenopus laevis oocytes. *Proc. Natl. Acad. Sci. U. S. A.* **2011**, *108*, 4334−4339.

(7) Zhu, L.; Brangwynne, C. P. Nuclear bodies: the emerging biophysics of nucleoplasmic phases. *Curr. Opin. Cell Biol.* **2015**, *34*, 23−30.

(8) Banani, S. F.; Lee, H. O.; Hyman, A. A.; Rosen, M. K. Biomolecular condensates: Organizers of cellular biochemistry. *Nat. Rev. Mol. Cell Biol.* **2017**, *18*, 285−298.

(9) Choi, J. M.; Holehouse, A. S.; Pappu, R. V. Physical Principles Underlying the Complex Biology of Intracellular Phase Transitions. *Annual Review of Biophysics* **2020**, *49*, 107−133.

(10) Bhat, P.; Honson, D.; Guttman, M. Nuclear compartmentalization as a mechanism of quantitative control of gene expression. *Nat. Rev. Mol. Cell Biol.* **2021**, *22*, 653−670.

(11) Alberti, S.; Hyman, A. A. Biomolecular condensates at the nexus of cellular stress, protein aggregation disease and ageing. *Nat. Rev. Mol. Cell Biol.* **2021**, *22*, 196−213.

(12) Shin, Y.; Berry, J.; Pannucci, N.; Haataja, M. P.; Toettcher, J. E.; Brangwynne, C. P. Spatiotemporal Control of Intracellular Phase Transitions Using Light-Activated optoDroplets. *Cell* **2017**, *168*, 159−171.e14.

(13) Jawerth, L.; Fischer-Friedrich, E.; Saha, S.; Wang, J.; Franzmann, T.; Zhang, X.; Sachweh, J.; Ruer, M.; Ijavi, M.; Saha, S.; Mahamid, J.; Hyman, A. A.; Jülicher, F. Protein condensates as aging Maxwell fluids. *Science* **2020**, *370*, 1317−1323.

(14) Alshareedah, I.; Moosa, M. M.; Pham, M.; Potoyan, D. A.; Banerjee, P. R. Programmable viscoelasticity in protein-RNA condensates with disordered sticker-spacer polypeptides. *Nat. Commun.* **2021**, *12*, 1−14.

(15) Ghosh, A.; Kota, D.; Zhou, H. X. Shear relaxation governs fusion dynamics of biomolecular condensates. *Nat. Commun.* **2021**, *12*, 1−10.

(16) de Gennes, P. G. *Scaling concepts in polymer physics*; Cornell University Press, 1979.

(17) Kato, M.; et al. Cell-free formation of RNA granules: Low complexity sequence domains form dynamic fibers within hydrogels. *Cell* **2012**, *149*, 753−767.

(18) Molliex, A.; Temirov, J.; Lee, J.; Coughlin, M.; Kanagaraj, A. P.; Kim, H. J.; Mittag, T.; Taylor, J. P. Phase Separation by Low Complexity Domains Promotes Stress Granule Assembly and Drives Pathological Fibrillization. *Cell* **2015**, *163*, 123−133.

(19) Kroschwald, S.; Maharana, S.; Mateju, D.; Malinovska, L.; Nüske, E.; Poser, I.; Richter, D.; Alberti, S. Promiscuous interactions and protein disaggregases determine the material state of stress-inducible RNP granules. *eLife* **2015**, *4*, 1−32.

(20) Patel, A.; et al. A Liquid-to-Solid Phase Transition of the ALS Protein FUS Accelerated by Disease Mutation. *Cell* **2015**, *162*, 1066−1077.

(21) Ronceray, P.; Zhang, Y.; Liu, X.; Wingreen, N. S. Stoichiometry Controls the Dynamics of Liquid Condensates of Associative Proteins. *Phys. Rev. Lett.* **2022**, *128*, 38102.

(22) Choi, J. M.; Hyman, A. A.; Pappu, R. V. Generalized models for bond percolation transitions of associative polymers. *Phys. Rev. E* **2020**, *102*, 1−6.

(23) Ryu, J.-K.; Bouchoux, C.; Liu, H. W.; Kim, E.; Minamino, M.; de Groot, R.; Katan, A. J.; Bonato, A.; Marenduzzo, D.; Michieletto, D.; Uhlmann, F.; Dekker, C. Bridging-induced phase separation induced by cohesin SMC protein complexes. *Science Advances* **2021**, *7*, eabe5905.

(24) Brackley, C. A.; Taylor, S.; Papantonis, A.; Cook, P. R.; Marenduzzo, D. Nonspecific bridging-induced attraction drives clustering of DNA-binding proteins and genome organization. *Proc. Natl. Acad. Sci. U.S.A.* **2013**, *110*, E3605−11.

(25) Ader, C.; Frey, S.; Maas, W.; Schmidt, H. B.; Görlich, D.; Baldus, M. Amyloid-like interactions within nucleoporin FG hydrogels. *Proc. Natl. Acad. Sci. U.S.A.* **2010**, *107*, 6281−6285.

(26) Shin, Y.; Brangwynne, C. P. Liquid phase condensation in cell physiology and disease. *Science* **2017**, *357*, 6537 DOI: 10.1126/science.aaf4382.

(27) Mathieu, C.; Pappu, R. V.; Taylor, J. P. Beyond aggregation: Pathological phase transitions in neurodegenerative disease. *Science* **2020**, *370*, 56−60.

(28) Nozawa, R. S.; Yamamoto, T.; Takahashi, M.; Tachiwana, H.; Maruyama, R.; Hirota, T.; Saitoh, N. Nuclear microenvironment in cancer: Control through liquid-liquid phase separation. *Cancer Science* **2020**, *111*, 3155−3163.

(29) Michieletto, D.; Gilbert, N. Role of nuclear RNA in regulating chromatin structure and transcription. *Curr. Opin. Cell Biol.* **2019**, *58*, 120−125.

(30) Matera, A. G. Cajal bodies. *Current biology* **2003**, *13*, 44106.

(31) Rino, J.; Carvalho, T.; Braga, J.; Desterro, J. M.; Lührmann, R.; Carmo-Fonseca, M. A stochastic view of spliceosome assembly and recycling in the nucleus. *PLoS Computational Biology* **2007**, *3*, 2019−2031.

(32) Brangwynne, C. P.; Tompa, P.; Pappu, R. V. Polymer physics of intracellular phase transitions. *Nature Phys.* **2015**, *11*, 899−904.

(33) Martin, E. W.; Mittag, T. Relationship of Sequence and Phase Separation in Protein Low-Complexity Regions. *Biochemistry* **2018**, *57*, 2478−2487.

(34) Wootton, J. C.; Federhen, S. Statistics of local complexity in amino acid sequences and sequence databases. *Computers and Chemistry* **1993**, *17*, 149−163.

(35) Martin, E. W.; Holehouse, A. S.; Peran, I.; Farag, M.; Incicco, J. J.; Bremer, A.; Grace, C. R.; Soranno, A.; Pappu, R. V.; Mittag, T. Valence and patterning of aromatic residues determine the phase behavior of prion-like domains. *Science* **2020**, *367*, 694−699.

(36) Romero, P.; Obradovic, Z.; Li, X.; Garner, E. C.; Brown, C. J.; Dunker, A. K. Sequence complexity of disordered protein. *Proteins: Struct., Funct., Bioinf.* **2001**, *42*, 38−48.

(37) van der Lee, R.; et al. Classification of Intrinsically Disordered Regions and Proteins. *Chem. Rev.* **2014**, *114*, 6589−6631.

(38) Nott, T. J.; Petsalaki, E.; Farber, P.; Jervis, D.; Fussner, E.; Plochowietz, A.; Craggs, T. D.; Bazett-Jones, D. P.; Pawson, T.; Forman-Kay, J. D.; Baldwin, A. J. Phase Transition of a Disordered Nuage Protein Generates Environmentally Responsive Membraneless Organelles. *Mol. Cell* **2015**, *57*, 936−947.

(39) Elbaum-Garfinkle, S.; Kim, Y.; Szczepaniak, K.; Chen, C. C. H.; Eckmann, C. R.; Myong, S.; Brangwynne, C. P. The disordered P granule protein LAF-1 drives phase separation into droplets with tunable viscosity and dynamics. *Proc. Natl. Acad. Sci. U.S.A.* **2015**, *112*, 7189−7194.

(40) Mitrea, D. M.; Cika, J. A.; Guy, C. S.; Ban, D.; Banerjee, P. R.; Stanley, C. B.; Nourse, A.; Deniz, A. A.; Kriwacki, R. W. Nucleophosmin integrates within the nucleolus via multi-modal interactions with proteins displaying R-rich linear motifs and rRNA. *eLife* **2016**, *5*, e13571.

(41) Murthy, A. C.; Dignon, G. L.; Kan, Y.; Zerze, G. H.; Parekh, S. H.; Mittal, J.; Fawzi, N. L. Molecular interactions underlying liquid-liquid phase separation of the FUS low-complexity domain. *Nature Structural & Molecular Biology* **2019**, *26*, 637−648.

(42) Lin, Y.; Currie, S. L.; Rosen, M. K. Intrinsically disordered sequences enable modulation of protein phase separation through distributed tyrosine motifs. *J. Biol. Chem.* **2017**, *292*, 19110−19120.

(43) Dignon, G. L.; Best, R. B.; Mittal, J. Biomolecular phase separation: From molecular driving forces to macroscopic properties. *Annu. Rev. Phys. Chem.* **2020**, *71*, 53−75.

(44) Chong, P. A.; Vernon, R. M.; Forman-Kay, J. D. RGG/RG Motif Regions in RNA Binding and Phase Separation. *J. Mol. Biol.* **2018**, *430*, 4650−4665.

(45) Thandapani, P.; O'Connor, T. R.; Bailey, T. L.; Richard, S. Defining the RGG/RG Motif. *Mol. Cell* **2013**, *50*, 613−623.

(46) Brady, J. P.; Farber, P. J.; Sekhar, A.; Lin, Y.-H.; Huang, R.; Bah, A.; Nott, T. J.; Chan, H. S.; Baldwin, A. J.; Forman-Kay, J. D.; Kay, L. E. Structural and hydrodynamic properties of an intrinsically disordered region of a germ cell-specific protein on phase separation. *Proc. Natl. Acad. Sci. U. S. A.* **2017**, *114*, E8194−E8203.

(47) Altmeyer, M.; Neelsen, K. J.; Teloni, F.; Pozdnyakova, I.; Grøfte, M.; Rask, M.-B. D.; Streicher, W.; Jungmichel, S.; Nielsen, M. L.; Lukas, J. Liquid demixing of intrinsically disordered proteins is seeded by poly(ADP-ribose). *Nat. Commun.* **2015**, *6*, 8088.

(48) Tsang, B.; Arsenault, J.; Vernon, R. M.; Lin, H.; Sonenberg, N.; Wang, L.-Y.; Bah, A.; Forman-Kay, J. D. Phosphoregulated FMRP phase separation models activity-dependent translation through bidirectional control of mRNA granule formation. *Proc. Natl. Acad. Sci. U. S. A.* **2019**, *116*, 4218−4227.

(49) Boeynaems, S.; et al. Phase Separation of < em > C9orf72 < em > Dipeptide Repeats Perturbs Stress Granule Dynamics. *Mol. Cell* **2017**, *65*, 1044−1055.e5.

(50) Saha, S.; Weber, C. A.; Nousch, M.; Adame-Arana, O.; Hoege, C.; Hein, M. Y.; Osborne-Nishimura, E.; Mahamid, J.; Jahnel, M.; Jawerth, L.; Pozniakovski, A.; Eckmann, C. R. Jülicher, F.; Hyman, A. A. Polar Positioning of Phase-Separated Liquid Compartments in Cells Regulated by an mRNA Competition Mechanism. *Cell* **2016**, *166*, 1572−1584.e16.

(51) Arribas-Layton, M.; Dennis, J.; Bennett, E. J.; Damgaard, C. K.; Lykke-Andersen, J. The RGG C-Terminal Domain of Human Lsm4 Promotes Processing Body Formation Stimulated by Arginine Dimethylation. *Mol. Cell. Biol.* **2016**, *36*, 2226−2235.

(52) Lin, Y.-H.; Forman-Kay, J. D.; Chan, H. S. Sequence-Specific Polyampholyte Phase Separation in Membraneless Organelles. *Phys. Rev. Lett.* **2016**, *117*, 178101.

(53) Das, R. K.; Pappu, R. V. Conformations of intrinsically disordered proteins are influenced by linear sequence distributions of oppositely charged residues. *Proc. Natl. Acad. Sci. U. S. A.* **2013**, *110*, 13392−13397.

(54) Anbarasu, A.; Anand, S.; Mathew, L.; Sethumadhavan, R. Influence of cation-p interactions on RNA-binding proteins. *Int. J. Biol. Macromol.* **2007**, *40*, 479−483.

(55) Zhang, H.; Li, C.; Yang, F.; Su, J.; Tan, J.; Zhang, X.; Wang, C. Cation-pi interactions at non-redundant protein-RNA interfaces. *Biochemistry (Moscow)* **2014**, *79*, 643−652.

(56) Alberti, S. Phase separation in biology. *Curr. Biol.* **2017**, *27*, R1097−R1102.

(57) Wu, H.; Fuxreiter, M. The Structure and Dynamics of Higher-Order Assemblies: Amyloids, Signalosomes, and Granules. *Cell* **2016**, *165*, 1055−1066.

(58) Martin, E. W.; Thomasen, F. E.; Milkovic, N. M.; Cuneo, M. J.; Grace, C.; Nourse, A.; Lindorff-Larsen, K.; Mittag, T. Interplay of folded domains and the disordered low-complexity domain in mediating hnRNPA1 phase separation. *Nucleic Acids Res.* **2021**, *49*, 2931−2945.

(59) Nozawa, R.-S.; Boteva, L.; Soares, D. C.; Naughton, C.; Dun, A. R.; Ramsahoye, B.; Bruton, P. C.; Saleeb, R. S.; Arnedo, M.; Hill, B.; Duncan, R.; Maciver, S. K.; Gilbert, N. SAF-A regulates interphase chromosome structure through oligomerisation with chromatin-associated RNAs. *Cell* **2017**, *169*, 1214−1227.e18.

(60) Marenda, M.; Lazarova, E.; Gilbert, N. The role of SAF-A/hnRNP U in regulating chromatin structure. *Current Opinion in Genetics & Development* **2022**, *72*, 38−44.

(61) Marenda, M.; Lazarova, E.; van de Linde, S.; Gilbert, N.; Michieletto, D. SuperStructure: a Parameter-Free Super-Structure Identifier for SMLM Data. *J. Cell Biol.* **2020**, DOI: 10.1101/2020.08.19.254540.

(62) Furst, E.; Squires, T. *Microrheology*; Oxford University Press, 2018.

(63) Boija, A.; et al. Transcription Factors Activate Genes through the Phase-Separation Capacity of Their Activation Domains. *Cell* **2018**, 1−14.

(64) Sabari, B. R. Coactivator condensation at super-enhancers links phase separation and gene control. *Science* **2018**, DOI: 10.1126/science.aar3958.

(65) Cho, W.-K.; Spille, J.-H.; Hecht, M.; Lee, C.; Li, C.; Grube, V.; Cisse, I. I. Mediator and RNA polymerase II clusters associate in transcription-dependent condensates. *Science* **2018**, *361*, 412−415.

(66) Strom, A. R.; Emelyanov, A. V.; Mir, M.; Fyodorov, D. V.; Darzacq, X.; Karpen, G. H. Phase separation drives heterochromatin domain formation. *Nature* **2017**, *547*, 241−245.

(67) Eeftens, J. M.; Kapoor, M.; Michieletto, D.; Brangwynne, C. P. Polycomb condensates can promote epigenetic marks but are not required for sustained chromatin compaction. *Nat. Commun.* **2021**, *12*, 5888 DOI: 10.1038/s41467-021-26147-5.

(68) Michieletto, D.; Gilbert, N. Role of nuclear RNA in regulating chromatin structure and transcription. *Curr. Opin. Cell Biol.* **2019**, *58*, 120−125.

(69) Jawerth, L. M.; Ijavi, M.; Ruer, M.; Saha, S.; Jahnel, M.; Hyman, A. A.; Jülicher, F.; Fischer-Friedrich, E. Salt-Dependent Rheology and Surface Tension of Protein Condensates Using Optical Traps. *Phys. Rev. Lett.* **2018**, *121*, 258101.

(70) Baum, M.; Erdel, F.; Wachsmuth, M.; Rippe, K. Retrieving the intracellular topology from multi-scale protein mobility mapping in living cells. *Nat. Commun.* **2014**, *5*, 4494.

(71) Celedon, A.; Hale, C. M.; Wirtz, D. Magnetic manipulation of nanorods in the nucleus of living cells. *Biophys. J.* **2011**, *101*, 1880−1886.

(72) Tseng, Y.; Lee, J. S.; Kole, T. P.; Jiang, I.; Wirtz, D. Micro-organization and visco-elasticity of the interphase nucleus revealed by particle nanotracking. *Journal of Cell Science* **2004**, *117*, 2159−2167.

(73) De Vries, A. H.; Krenn, B. E.; Van Driel, R.; Subramaniam, V.; Kanger, J. S. Direct observation of nanomechanical properties of chromatin in living cells. *Nano Lett.* **2007**, *7*, 1424−1427.

(74) Caragine, C. M.; Haley, S. C.; Zidovska, A. Surface Fluctuations and Coalescence of Nucleolar Droplets in the Human Cell Nucleus. *Phys. Rev. Lett.* **2018**, *121*, 148101.

(75) Gopal, P. P.; Nirschl, J. J.; Klinman, E.; Holzbaur, E. L. F. Amyotrophic lateral sclerosis-linked mutations increase the viscosity of liquid-like TDP-43 RNP granules in neurons. *Proc. Natl. Acad. Sci. U. S. A.* **2017**, *114*, E2466−E2475.

(76) Wang, H.; Kelley, F. M.; Milovanovic, D.; Schuster, B. S.; Shi, Z. Surface tension and viscosity of protein condensates quantified by micropipette aspiration. *Biophysical Reports* **2021**, *1*, 100011.

(77) Patel, A.; et al. A Liquid-to-Solid Phase Transition of the ALS Protein FUS Accelerated by Disease Mutation. *Cell* **2015**, *162*, 1066−1077.

(78) Ijavi, M.; Style, R. W.; Emmanouilidis, L.; Kumar, A.; Meier, S. M.; Torzynski, A. L.; Allain, F. H.; Barral, Y.; Steinmetz, M. O.; Dufresne, E. R. Surface tensiometry of phase separated protein and polymer droplets by the sessile drop method. *Soft Matter* **2021**, *17*, 1655−1662.

(79) Görisch, S. M.; Wachsmuth, M.; Tóth, K. F.; Lichter, P.; Rippe, K. Histone acetylation increases chromatin accessibility. *Journal of Cell Science* **2005**, *118*, 5825−5834.

(80) Mason, T. G.; Weitz, D. A. Optical measurements of frequency-dependent linear viscoelastic moduli of complex fluids. *Phys. Rev. Lett.* **1995**, *74*, 1250−1253.

(81) Kasza, K. E.; Rowat, A. C.; Liu, J.; Angelini, T. E.; Brangwynne, C. P.; Koenderink, G. H.; Weitz, D. A. The cell as a material. *Curr. Opin. Cell Biol.* **2007**, *19*, 101−107.

(82) Wirtz, D. Particle-Tracking Microrheology of Living Cells: Principles and Applications. *Annual Review of Biophysics* **2009**, *38*, 301−326.

(83) Hameed, F. M.; Rao, M.; Shivashankar, G. V. Dynamics of Passive and Active Particles in the Cell Nucleus. *PLoS One* **2012**, *7*, 1−11.

(84) Fitzpatrick, R.; Michieletto, D.; Peddireddy, K. R.; Hauer, C.; Kyrillos, C.; Gurmessa, B. J.; Robertson-anderson, R. M. Synergistic Interactions Between DNA and Actin Trigger Emergent Viscoelastic Behavior. *Phys. Rev. Lett.* **2018**, *121*, 257801.

(85) Tassieri, M.; Evans, R. M.; Warren, R. L.; Bailey, N. J.; Cooper, J. M. Microrheology with optical tweezers: Data analysis. *New J. Phys.* **2012**, *14*.115032

(86) Evans, R. M.; Tassieri, M.; Auhl, D.; Waigh, T. A. Direct conversion of rheological compliance measurements into storage and loss moduli. *Physical Review E - Statistical, Nonlinear, and Soft Matter Physics* **2009**, *80*, 8−11.

(87) Crocker, J.; Grier, D. Methods of Digital Video Microscopy for Colloidal Studies. *J. Colloid Interface Sci.* **1996**, *179*, 298−310.

(88) Tinevez, J. Y.; Perry, N.; Schindelin, J.; Hoopes, G. M.; Reynolds, G. D.; Laplantine, E.; Bednarek, S. Y.; Shorte, S. L.; Eliceiri, K. W. TrackMate: An open and extensible platform for single-particle tracking. *Methods* **2017**, *115*, 80−90.

(89) Mason, T. G. Estimating the viscoelastic moduli of complex fluids using the generalized Stokes-Einstein equation. *Rheol. Acta* **2000**, *39*, 371−378.

(90) Savin, T.; Doyle, P. S. Static and dynamic errors in particle tracking microrheology. *Biophys. J.* **2005**, *88*, 623−638.

(91) Ciccone, G.; Dobre, O.; Gibson, G. M.; Rey, J. M.; Gonzalez-Garcia, C.; Vassalli, M.; Salmeron-Sanchez, M.; Tassieri, M. What Caging Force Cells Feel in 3D Hydrogels: A Rheological Perspective. *Adv. Healthcare Mater.* **2020**, *9*, 1−6.

(92) Martinez, V. A.; Besseling, R.; Croze, O. A.; Tailleur, J.; Reufer, M.; Schwarz-Linek, J.; Wilson, L. G.; Bees, M. A.; Poon, W. C. Differential dynamic microscopy: A high-throughput method for characterizing the motility of microorganisms. *Biophys. J.* **2012**, *103*, 1637−1647.

(93) Cerbino, R.; Trappe, V. Differential dynamic microscopy: Probing wave vector dependent dynamics with a microscope. *Phys. Rev. Lett.* **2008**, *100*, 1−4.

(94) Edera, P.; Bergamini, D.; Trappe, V.; Giavazzi, F.; Cerbino, R. Differential dynamic microscopy microrheology of soft materials: A tracking-free determination of the frequency-dependent loss and storage moduli. *Physical Review Materials* **2017**, *1*, 1−11.

(95) Smrek, J.; Garamella, J.; Robertson-Anderson, R.; Michieletto, D. Topological tuning of DNA mobility in entangled solutions of supercoiled plasmids. *Science Advances* **2021**, *7*, 1−28.

(96) Chapman, C. D.; Robertson-Anderson, R. M. Nonlinear microrheology reveals entanglement-driven molecular-level viscoelasticity of concentrated DNA. *Phys. Rev. Lett.* **2014**, *113*, 1−5.

(97) Soumpasis, D. M. Theoretical analysis of fluorescence photobleaching recovery experiments. *Biophys. J.* **1983**, *41*, 95−97.

(98) Axelrod, D.; Koppel, D. E.; Schlessinger, J.; Elson, E.; Webb, W. W. Mobility measurement by analysis of fluorescence photobleaching recovery kinetics. *Biophys. J.* **1976**, *16*, 1055−1069.

(99) Mueller, F.; Wach, P.; McNally, J. G. Evidence for a common mode of transcription factor interaction with chromatin as revealed by improved quantitative fluorescence recovery after photobleaching. *Biophys. J.* **2008**, *94*, 3323−3339.

(100) Mazza, D.; Abernathy, A.; Golob, N.; Morisaki, T.; McNally, J. G. A benchmark for chromatin binding measurements in live cells. *Nucleic Acids Res.* **2012**, *40*, 1−13.

(101) Taylor, N. O.; Wei, M. T.; Stone, H. A.; Brangwynne, C. P. Quantifying Dynamics in Phase-Separated Condensates Using Fluorescence Recovery after Photobleaching. *Biophys. J.* **2019**, *117*, 1285−1300.

(102) Elbaum-Garfinkle, S.; Kim, Y.; Szczepaniak, K.; Chen, C. C. H.; Eckmann, C. R.; Myong, S.; Brangwynne, C. P. The disordered P granule protein LAF-1 drives phase separation into droplets with tunable viscosity and dynamics. *Proc. Natl. Acad. Sci. U.S.A.* **2015**, *112*, 7189−7194.

(103) Milles, S.; Tyagi, S.; Banterle, N.; Koehler, C.; Vandelinder, V.; Plass, T.; Neal, A. P.; Lemke, E. A. Click strategies for single-molecule protein fluorescence. *J. Am. Chem. Soc.* **2012**, *134*, 5187−5195.

(104) Keenen, M. M.; Brown, D.; Brennan, L. D.; Renger, R.; Khoo, H.; Carlson, C. R.; Huang, B.; Grill, S. W.; Narlikar, G. J.; Redding, S. HP1 proteins compact dna into mechanically and positionally stable phase separated domains. *eLife* **2021**, *10*, 1−38.

(105) Muzzopappa, F.; Hertzog, M.; Erdel, F. DNA length tunes the fluidity of DNA-based condensates. *Biophys. J.* **2021**, *120*, 1288−1300.

(106) Langowski, J. Protein-Protein Interactions Determined by Fluorescence Correlation Spectroscopy. *Methods in Cell Biology* **2008**, *85*, 471−484.

(107) Elson, E. L.; Magde, D. Fluorescence correlation spectroscopy. I. Conceptual basis and theory. *Biopolymers* **1974**, *13*, 1−27.

(108) Tian, Y.; Martinez, M. M.; Pappas, D. Fluorescence correlation spectroscopy: A review of biochemical and microfluidic applications. *Appl. Spectrosc.* **2011**, *65*, 115−124.

(109) Yu, L.; Lei, Y.; Ma, Y.; Liu, M.; Zheng, J.; Dan, D.; Gao, P.; Comprehensive, A. Review of Fluorescence Correlation Spectroscopy. *Frontiers in Physics* **2021**, *9*, 1−21.

(110) Bracha, D.; Walls, M. T.; Wei, M. T.; Zhu, L.; Kurian, M.; Avalos, J. L.; Toettcher, J. E.; Brangwynne, C. P. Mapping Local and Global Liquid Phase Behavior in Living Cells Using Photo-Oligomerizable Seeds. *Cell* **2018**, *175*, 1467−1480.e13.

(111) Alshareedah, I.; Thurston, G. M.; Banerjee, P. R. Quantifying viscosity and surface tension of multicomponent protein-nucleic acid condensates. *Biophys. J.* **2021**, *120*, 1161−1169.

(112) Alshareedah, I.; Moosa, M. M.; Raju, M.; Potoyan, D. A.; Banerjee, P. R. Phase transition of RNA-protein complexes into ordered hollow condensates. *Proc. Natl. Acad. Sci. U.S.A.* **2020**, *117*, 15650−15658.

(113) Maharana, S.; et al. RNA buffers the phase separation behavior of prion-like RNA binding proteins. *Science* **2018**, *360*, 918−921.

(114) Di Rienzo, S.; Piazza, V.; Gratton, E.; Beltram, F.; Cardarelli, F. Probing short-range protein Brownian motion in the cytoplasm of living cells. *Nat. Commun.* **2014**, *5*, 1−8.

(115) McSwiggen, D. T.; Hansen, A. S.; Teves, S. S.; Marie-Nelly, H.; Hao, Y.; Heckert, A. B.; Umemoto, K. K.; Dugast-Darzacq, C.; Tjian, R.; Darzacq, X. Evidence for DNA-mediated nuclear compartmentalization distinct from phase separation. *eLife* **2019**, *8*, 1−31.

(116) Izeddin, I.; Récamier, V.; Bosanac, L.; Cissé, I. I.; Boudarene, L.; Dugast-Darzacq, C.; Proux, F.; Bénichou, O.; Voituriez, R.; Bensaude, O.; Dahan, M.; Darzacq, X. Single-molecule tracking in live cells reveals distinct target-search strategies of transcription factors in the nucleus. *eLife* **2014**, *2014*, 1−27.

(117) Cho, W. K.; Jayanth, N.; English, B. P.; Inoue, T.; Andrews, J. O.; Conway, W.; Grimm, J. B.; Spille, J. H.; Lavis, L. D.; Lionnet, T.; Cisse, I. I.; Polymerase, R. N. A., II cluster dynamics predict mRNA output in living cells. *eLife* **2016**, *5*, 1−31.

(118) Cho, W. K.; Spille, J. H.; Hecht, M.; Lee, C.; Li, C.; Grube, V.; Cisse, I. I. Mediator and RNA polymerase II clusters associate in transcription-dependent condensates. *Science* **2018**, *361*, 412−415.

(119) Hilbert, L.; Sato, Y.; Kuznetsova, K.; Bianucci, T.; Kimura, H.; Jülicher, F.; Honigmann, A.; Zaburdaev, V.; Vastenhouw, N. L. Transcription organizes euchromatin via microphase separation. *Nat. Commun.* **2021**, *12*, 1−12.

(120) Pancholi, A.; Klingberg, T.; Zhang, W.; Prizak, R.; Mamontova, I.; Noa, A.; Sobucki, M.; Kobitski, A. Y.; Nienhaus, G. U.; Zaburdaev, V.; Hilbert, L. RNA polymerase II clusters form in line with surface condensation on regulatory chromatin. *Molecular Systems Biology* **2021**, *17*, 1−26.

(121) Chaikin, P.; Lubensky, T. *Principles of Condensed Matter Physics*; Cambridge University Press, 2000.

(122) Rosowski, K. A.; Vidal-Henriquez, E.; Zwicker, D.; Style, R. W.; Dufresne, E. R. Elastic stresses reverse Ostwald ripening. *Soft Matter* **2020**, *16*, 5892−5897.

(123) Michieletto, D.; Gilbert, N. Role of nuclear RNA in regulating chromatin structure and transcription. *Curr. Opin. Cell Biol.* **2019**, *58*, 120−125.

(124) Lee, D. S.; Wingreen, N. S.; Brangwynne, C. P. Chromatin mechanics dictates subdiffusion and coarsening dynamics of embedded condensates. *Nat. Phys.* **2021**, *17*, 531−538.

(125) Halverson, J. D.; Smrek, J.; Kremer, K.; Grosberg, A. From a melt of rings to chromosome territories: the role of topological constraints in genome folding. *Rep. Prog. Phys.* **2014**, *77*, 022601.

(126) Style, R. W.; Sai, T.; Fanelli, N.; Ijavi, M.; Smith-Mannschott, K.; Xu, Q.; Wilen, L. A.; Dufresne, E. R. Liquid-Liquid Phase Separation in an Elastic Network. *Physical Review X* **2018**, *8*, 11028.

(127) Fernández-Rico, C.; Sai, T.; Sicher, A.; Style, R. W.; Dufresne, E. R. Putting the Squeeze on Phase Separation. *JACS Au* **2022**, *2*, 66−73.

(128) Kaur, T.; Alshareedah, I.; Wang, W.; Ngo, J.; Moosa, M. M.; Banerjee, P. R. Molecular crowding tunes material states of ribonucleoprotein condensates. *Biomolecules* **2019**, *9*, 1−17.

(129) Patel, A.; et al. A Liquid-to-Solid Phase Transition of the ALS Protein FUS Accelerated by Disease Mutation. *Cell* **2015**, *162*, 1066−1077.

(130) Wang, J.; Choi, J. M.; Holehouse, A. S.; Lee, H. O.; Zhang, X.; Jahnel, M.; Maharana, S.; Lemaitre, R.; Pozniakovsky, A.; Drechsel, D.; Poser, I.; Pappu, R. V.; Alberti, S.; Hyman, A. A. A Molecular Grammar Governing the Driving Forces for Phase Separation of Prion-like RNA Binding Proteins. *Cell* **2018**, *174*, 688−699.e16.

(131) Ghosh, A.; Zhou, H. X. Determinants for Fusion Speed of Biomolecular Droplets. *Angewandte Chemie - International Edition* **2020**, *59*, 20837−20840.

(132) Alshareedah, I.; Kaur, T.; Banerjee, P. R. *Methods in Enzymology*, 1st ed.; Elsevier Inc., 2021; Vol. *646*; pp 143−183.

(133) Peng, A.; Weber, S. C. Evidence for and against liquid-liquid phase separation in the nucleus. *Non-coding RNA* **2019**, DOI: 10.3390/ncrna5040050.

(134) McSwiggen, D. T.; Mir, M.; Darzacq, X.; Tjian, R. Evaluating phase separation in live cells: diagnosis, caveats, and functional consequences. *Genes & development* **2019**, *33*, 1619−1634.

(135) Brackley, C. A.; Liebchen, B.; Michieletto, D.; Mouvet, F.; Cook, P. R.; Marenduzzo, D. Ephemeral Protein Binding to DNA Shapes Stable Nuclear Bodies and Chromatin Domains. *Biophys. J.* **2017**, *112*, 1085−1093.

(136) Brackey, C. A.; Marenduzzo, D.; Gilbert, N. Mechanistic modeling of chromatin folding to understand function. *Nat. Methods* **2020**, *17*, 767−775.

(137) Erdel, F.; Rippe, K. Formation of Chromatin Subcompartments by Phase Separation. *Biophys. J.* **2018**, *114*, 2262−2270.

(138) Rubinstein, M.; Semenov, A. N. Dynamics of entangled solutions of associating polymers. *Macromolecules* **2001**, *34*, 1058−1068.

(139) Michieletto, D.; Colì, D.; Marenduzzo, D.; Orlandini, E. Nonequilibrium Theory of Epigenomic Microphase Separation in the Cell Nucleus. *Phys. Rev. Lett.* **2019**, *123*, 831396.

(140) Brackley, C. A.; Johnson, J.; Kelly, S.; Cook, P. R.; Marenduzzo, D. Simulated binding of transcription factors to active and inactive regions folds human chromosomes into loops, rosettes and topological domains. *Nucleic Acids Res.* **2016**, *44*, 3503−3512.

(141) Khanna, N.; Zhang, Y.; Lucas, J. S.; Dudko, O. K.; Murre, C. Chromosome dynamics near the sol-gel phase transition dictate the timing of remote genomic interactions. *Nat. Commun.* **2019**, *10*, 1−13.

(142) Rubinstein, M.; Colby, H. R. *Polymer Physics*; Oxford University Press, 2003.

(143) Cahn, J. W.; Hilliard, J. E. Free energy of a nonuniform system. I. Interfacial Free Energy. *J. Chem. Phys.* **1959**, *30*, 1121−1124.

(144) Colì, D.; Orlandini, E.; Michieletto, D.; Marenduzzo, D. Magnetic polymer models for epigenetics-driven chromosome folding. *Phys. Rev. E* **2019**, *100*, 1−10.

(145) Narayanan, A.; Meriin, A.; Owen Andrews, J.; Spille, J. H.; Sherman, M. Y.; Cisse, I. I. A first order phase transition mechanism underlies protein aggregation in mammalian cells. *eLife* **2019**, *8*, 1−26.

(146) Zwicker, D.; Baumgart, J.; Redemann, S.; Müller-Reichert, T.; Hyman, A. A.; Jülicher, F. Positioning of Particles in Active Droplets. *Phys. Rev. Lett.* **2018**, *121*, 158102.

(147) Zwicker, D.; Decker, M.; Jaensch, S.; Hyman, A. A.; Jülicher, F. Centrosomes are autocatalytic droplets of pericentriolar material organized by centrioles. *Proc. Natl. Acad. Sci. U.S.A.* **2014**, *111*, E2636−E2645.

(148) Zwicker, D.; Hyman, A. A.; Jülicher, F. Suppression of Ostwald ripening in active emulsions. *Phys. Rev. E* **2015**, *92*, 1−13.

(149) Shin, Y.; Chang, Y. C.; Lee, D. S.; Berry, J.; Sanders, D. W.; Ronceray, P.; Wingreen, N. S.; Haataja, M.; Brangwynne, C. P. Liquid Nuclear Condensates Mechanically Sense and Restructure the Genome. *Cell* **2018**, *175*, 1481−1491.e13.

(150) Posey, A. E.; Holehouse, A. S.; Pappu, R. V. *Methods in Enzymology*, 1st ed.; Elsevier, Inc., 2018; Vol. *611*; pp 1−30.

(151) Dignon, G. L.; Zheng, W.; Best, R. B.; Kim, Y. C.; Mittal, J. Relation between single-molecule properties and phase behavior of intrinsically disordered proteins. *Proc. Natl. Acad. Sci. U.S.A.* **2018**, *115*, 9929−9934.

(152) Dignon, G. L.; Zheng, W.; Kim, Y. C.; Mittal, J. Temperature-Controlled Liquid-Liquid Phase Separation of Disordered Proteins. *ACS Central Science* **2019**, *5*, 821−830.

(153) Dignon, G. L.; Zheng, W.; Kim, Y. C.; Best, R. B.; Mittal, J. Sequence determinants of protein phase behavior from a coarse-grained model. *PLoS Computational Biology* **2018**, *14*, 1−23.

(154) Joseph, J. A.; Reinhardt, A.; Aguirre, A.; Chew, P. Y.; Russell, K. O.; Espinosa, J. R.; Garaizar, A.; Collepardo-Guevara, R. Physics-

driven coarse-grained model for biomolecular phase separation with near-quantitative accuracy. *Nature Computational Science* **2021**, *1*, 732−743.

(155) Michieletto, D.; Orlandini, E.; Marenduzzo, D. Polymer model with Epigenetic Recoloring Reveals a Pathway for the de novo Establishment and 3D Organization of Chromatin Domains. *Physical Review X* **2016**, *6*, 041047.

(156) Di Pierro, M.; Zhang, B.; Aiden, E. L.; Wolynes, P. G.; Onuchic, J. N. Transferable model for chromosome architecture. *Proc. Natl. Acad. Sci. U. S. A.* **2016**, *113*, 12168−12173.

(157) Sabari, B. R. et al. Coactivator condensation at super-enhancers links phase separation and gene control. *Science* **2018**, *361*. DOI: 10.1126/science.aar3958